FOREST ECOLOGY

Impacts of species richness on productivity in a large-scale subtropical forest experiment

Yuanyuan Huang[1]*, Yuxin Chen[1]*, Nadia Castro-Izaguirre[1], Martin Baruffol[1,2], Matteo Brezzi[1]†, Anne Lang[3], Ying Li[3], Werner Härdtle[3], Goddert von Oheimb[4,5], Xuefei Yang[6,7], Xiaojuan Liu[1,8], Kequan Pei[8], Sabine Both[6], Bo Yang[9], David Eichenberg[6,10], Thorsten Assmann[3], Jürgen Bauhus[11], Thorsten Behrens[12], François Buscot[4,13], Xiao-Yong Chen[14], Douglas Chesters[15], Bing-Yang Ding[16], Walter Durka[4,17], Alexandra Erfmeier[4,18], Jingyun Fang[19], Markus Fischer[20], Liang-Dong Guo[21], Dali Guo[22]†, Jessica L. M. Gutknecht[23], Jin-Sheng He[19], Chun-Ling He[15], Andy Hector[24], Lydia Hönig[6], Ren-Yong Hu[25], Alexandra-Maria Klein[26], Peter Kühn[12], Yu Liang[8], Shan Li[8], Stefan Michalski[17], Michael Scherer-Lorenzen[27], Karsten Schmidt[12], Thomas Scholten[12], Andreas Schuldt[3,4], Xuezheng Shi[28], Man-Zhi Tan[28], Zhiyao Tang[19], Stefan Trogisch[4,6,27], Zhengwen Wang[29], Erik Welk[4,6], Christian Wirth[4,10], Tesfaye Wubet[4,13], Wenhua Xiang[30], Mingjian Yu[31], Xiao-Dong Yu[15], Jiayong Zhang[32], Shouren Zhang[8], Naili Zhang[8], Hong-Zhang Zhou[15], Chao-Dong Zhu[15], Li Zhu[8], Helge Bruelheide[4,6]‡, Keping Ma[8]‡, Pascal A. Niklaus[1]‡, Bernhard Schmid[1]‡

Biodiversity experiments have shown that species loss reduces ecosystem functioning in grassland. To test whether this result can be extrapolated to forests, the main contributors to terrestrial primary productivity, requires large-scale experiments. We manipulated tree species richness by planting more than 150,000 trees in plots with 1 to 16 species. Simulating multiple extinction scenarios, we found that richness strongly increased stand-level productivity. After 8 years, 16-species mixtures had accumulated over twice the amount of carbon found in average monocultures and similar amounts as those of two commercial monocultures. Species richness effects were strongly associated with functional and phylogenetic diversity. A shrub addition treatment reduced tree productivity, but this reduction was smaller at high shrub species richness. Our results encourage multispecies afforestation strategies to restore biodiversity and mitigate climate change.

Forest ecosystems harbor around two-thirds of all terrestrial plant species. Observational studies suggest that species-rich forests exceed the productivity of less diverse forests (*1*–*3*), but covarying factors [such as spatial heterogeneity in abiotic environment (*1*), species composition (*2*), and successional stages (*2*)] make assigning causation difficult. Systematic experimental manipulations of plant species composition in grassland (*4*–*6*) have shown that plant diversity promotes community productivity through niche partitioning among species, specifically with respect to abiotic resources (*7*) or interactions with enemies (*8*), or through increasing the contribution of highly productive species in more diverse communities (*9*). These two types of biological mechanisms are thought to be captured by the complementarity and selection effects calculated by the additive partitioning of net biodiversity effects (*10*). Complementarity effects are large and positive when most species in a mixture contribute more than expected on the basis of their monoculture values to community values, and negative when most species in a mixture contribute less than expected, whereas selection effects are large when a single or few species show a disproportionate contribution to community values (*10*). It has been postulated that biodiversity effects may be weak or absent in forests, especially in those of high species richness, because the coexistence of so many species may require similar niches and competitive abilities (*1*, *11*–*13*).

Several forest biodiversity experiments have recently been initiated (*14*, *15*), mostly in the temperate zone or in small plots with limited species richness gradients (*16*–*22*). Here, we report results of the "BEF-China" experiment (BEF, biodiversity–ecosystem functioning) that was established in a highly diverse subtropical forest in southeast China (*23*). The experiment is characterized by a large species richness gradient, multiple simulated extinction scenarios, high replication, and extended duration (2009 to present). We studied how changing tree species richness affected stand-level development of tree basal area, aboveground volume, and aboveground carbon (C) from 2013 to 2017 (*24*). The experiment was implemented at two sites (site A and site B) of ~20 ha each, with communities assembled from six partially overlapping species pools (three per site). A complete pool represented a 16-species community, which was repeatedly divided to yield reduced richness levels of eight, four, two, and one species; in addition, 24-species communities were created by combining species of all three pools present at each site (fig. S1) (*24*). Of the 42 tree species used in the experiment (table S1), 40 occurred with the same frequency at each richness level. The remaining two species were typical plantation species in the area and were established in reference monocultures. A special feature of the design is that within each pool, communities form nested series that simulate different trajectories of trait-based species extinctions (fig. S2 and table S2). We analyzed trajectories related to

[1]Department of Evolutionary Biology and Environmental Studies, University of Zürich, Winterthurerstrasse 190, 8057 Zürich, Switzerland. [2]Instituto de Investigación de Recursos Biológicos Alexander von Humboldt, calle 28A # 5-09, Bogotá DC, Colombia. [3]Institute of Ecology, Leuphana University of Lüneburg, Universitätsallee 1, 21335 Lüneburg, Germany. [4]German Centre for Integrative Biodiversity Research (iDiv) Halle–Jena–Leipzig, Deutscher Platz 5e, 04103 Leipzig, Germany. [5]Technische Universität Dresden, Institute of General Ecology and Environmental Protection, Post Office Box 1117, 01735 Tharandt, Germany. [6]Martin Luther University Halle-Wittenberg, Am Kirchtor 1, 06108 Halle (Saale), Germany. [7]Kunming Institute of Botany, Chinese Academy of Sciences, 134, Lanhei Road, Kunming, 650204, China. [8]State Key Laboratory of Vegetation and Environmental Change, Institute of Botany, Chinese Academy of Sciences, Beijing 100093, China. [9]Key Laboratory of Plant Resources and Biodiversity of Jiangxi Province, Jingdezhen University, 838 Cidu Avenue, Jingdezhen, Jiangxi 333000, China. [10]Institut für Spezielle Botanik und Funktionelle Biodiversität, University of Leipzig, 04103 Leipzig, Germany. [11]Chair of Silviculture, Faculty of Environment and Natural Resources, University of Freiburg, Tennenbacherstraße 4, 79106 Freiburg, Germany. [12]Department of Geosciences, Soil Science and Geomorphology, University of Tübingen, Rümelinstraße 19-23, 72074 Tübingen, Germany. [13]Helmholtz Centre for Environmental Research–UFZ, Department of Soil Ecology, Theodor-Lieser-Straße 4, 06120 Halle (Saale), Germany. [14]School of Ecological and Environmental Sciences, ECNU-UH Joint Translational Science and Technology Research Institute, East China Normal University, Shanghai 200241, China. [15]Institute of Zoology, Chinese Academy of Sciences, 1 Beichen West Road, Chaoyang District, Beijing 100101, China. [16]School of Life and Environment Sciences, Wenzhou University, Wenzhou, China. [17]Helmholtz Centre for Environmental Research–UFZ, Department of Community Ecology, Theodor-Lieser-Straße 4, 06120 Halle (Saale), Germany. [18]Institute for Ecosystem Research, Kiel University, Olshausenstraße 75, 24118 Kiel, Germany. [19]Department of Ecology, Peking University, 5 Yiheyuan Road, Beijing 100871, China. [20]Institute of Plant Sciences, University of Bern, Altenbergrain 21, 3013 Bern, Switzerland. [21]State Key Laboratory of Mycology, Institute of Microbiology, Chinese Academy of Sciences, Beijing 100101, China. [22]Institute of Geographic Sciences and Natural Resources Research, Chinese Academy of Sciences, Beijing, China. [23]Department of Soil, Water, and Climate University of Minnesota, Twin Cities, MN, USA. [24]Department of Plant Sciences, University of Oxford, South Parks Road, OX1 3RB, UK. [25]Department of Biology, College of Life and Environmental Sciences, Wenzhou University, Wenzhou 325035 China. [26]Nature Conservation and Landscape Ecology, Faculty of Earth and Environmental Sciences, University of Freiburg, Germany. [27]Geobotany, Faculty of Biology, University of Freiburg, Freiburg, Germany. [28]Institute of Soil Science, the Chinese Academy of Sciences, Nanjing 210008 China. [29]Institute of Applied Ecology, Chinese Academy of Sciences, 72 Wenhua Road, Shenyang 110016, P.R. China. [30]Faculty of Life Science and Technology, Central South University of Forestry and Technology, Changsha 410004, Hunan Province, China. [31]College of Life Sciences, Zhejiang University, Hangzhou, Zhejiang 310058, China. [32]Institute of Ecology, College of Chemistry and Life Science, Zhejiang Normal University, Yingbin Road No. 688, Jinhua City, Zhejiang Province, China 321004.
*These authors contributed equally to this work. †Deceased.
‡Corresponding author. Email: helge.bruelheide@botanik.uni-halle.de (H.B.); kpma@ibcas.ac.cn (K.M.); pascal.niklaus@ieu.uzh.ch (P.A.N.); bernhard.schmid@ieu.uzh.ch (B.S.)

means and diversities of the three functional traits leaf duration (LD), specific leaf area (SLA), and wood density (WD). These traits are often used to characterize plant-growth strategies (*25*) and are potentially related to extinction probabilities under environmental change (*26*). In 2009 (site A) and 2010 (site B), communities of 400 trees were planted on square plots 0.067 ha in size, which equals the Chinese area unit of 1 mu. Communities of pools A2, A3, B2, and B3 (fig. S1) were established in single 1-mu plots. Each community of pools A1 and B1 was replicated in five 1-mu plots, four of which formed a larger square plot of 4 mu; these four plots received an understory shrub species richness treatment factorially crossed with the tree species richness gradient: Plots had zero, two, four, or eight shrub species randomly selected from a pool of 18 species, with shrubs planted at the same density as the trees.

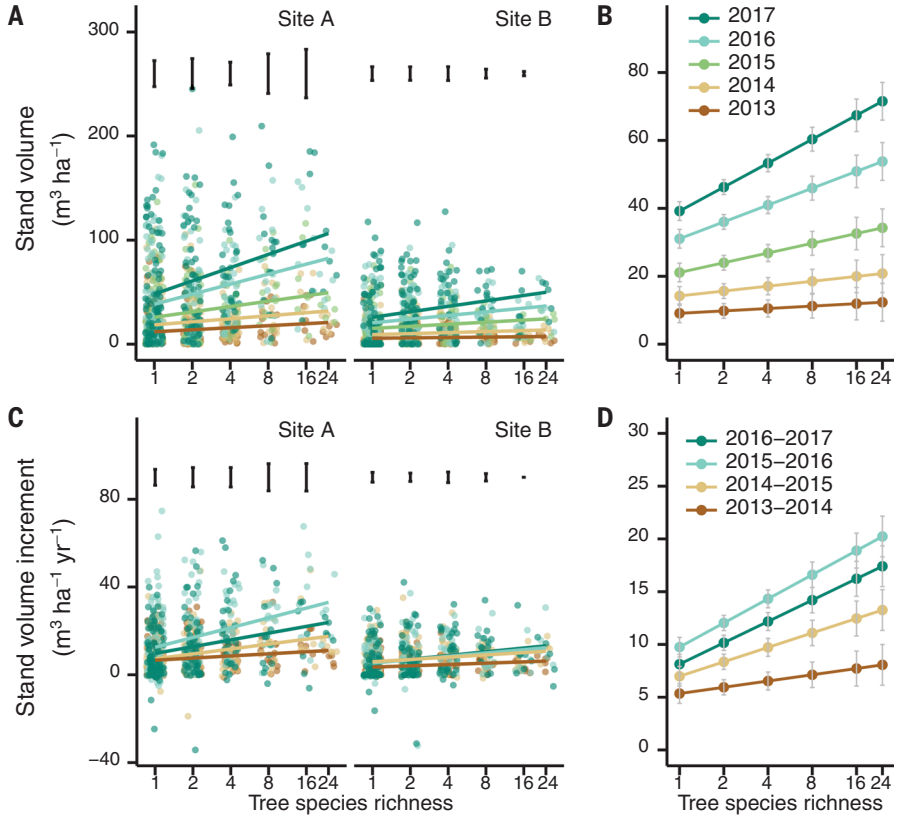

Fig. 1. Stand-level tree volume and its increment as a function of tree species richness from 2013 to 2017. (**A** and **B**) Stand-level tree volume. (**C** and **D**) Stand-level tree volume increment. In (A) and (C), raw data points and regression lines are shown for each year. (B) and (D) show predicted means and standard errors based on mixed-effects models (Table 1). The extremes of the point cloud taper off toward higher diversity levels because of decreasing sample size; quantile regressions show qualitatively the same positive relationships for the largest 10% of values at each diversity level (fig. S4). Standard deviations of species compositions (square root of corresponding between-composition variance components), shown as black error bars above the raw data, indicate that there is no variance-reduction effect of increasing species richness.

We found significant positive effects of the logarithm of tree species richness on stand basal area and stand volume as well as on the annual increments of these two variables (Table 1, Fig. 1, and figs. S3 and S4). These effects grew steadily through time (changes in stand volume per doubling of species, with standard errors, were 0.74 ± 0.58, 1.47 ± 0.85, 2.98 ± 1.29, 4.91 ± 1.83, and 6.99 ± 2.24 m^3 ha^{-1} from 2013 to 2017). Mean volume increments were larger in wetter years ($F_{1,99.1}$ = 7.58, P = 0.007), but richness effects on volume increments were not affected by annual precipitation ($F_{1,91.7}$ = 2.25, P = 0.137). After 8 years of growth (site A), the average 16-species mixture stored 31.5 Mg C ha^{-1} above ground [95% Bayesian credible interval (CI), 25.5 to 37.6] (*24*), which is more than double the amount found in monocultures (11.9 Mg C ha^{-1}; CI, 10.6 to 13.5) (fig. S5) and similar to the C storage of monocultures of the commercial plantation species *Cunninghamia lanceolata* (26.3 Mg C ha^{-1}; CI, 19.0 to 33.2) and *Pinus massoniana* (28.5 Mg C ha^{-1}; CI, 20.8 to 36.1) (fig. S5). These strong positive effects of tree species richness must have been driven by faster growth of live trees in more diverse stands because tree survival rate did not increase with species richness (fig. S6). This is in contrast to findings in a large grassland biodiversity experiment in which positive diversity effects on productivity were mediated by a greater number rather than larger size of individuals in high-diversity plots (*27*).

The net biodiversity effect (*10*) on stand volume increased through time for mixtures of all species-richness levels (year as linear term with $F_{1,38.6}$ = 29.15, P < 0.001) (Fig. 2) and was driven by increases in complementarity effects (year as linear term with $F_{1,52.4}$ = 9.23, P = 0.004) (Fig. 2). Selection effects were on average negative ($F_{1,37.8}$ = 8.75, P = 0.005) because some species with relatively high monoculture stand volume had lower performance in mixtures, and some with relatively low monoculture stand volume had higher performance. This was corroborated by negative species-level selection effects (fig. S7).

We tested whether the observed species-richness effects could be explained by functional or phylogenetic diversity. For this, we calculated functional diversity (FD) and functional dispersion (FDis) (*24*) on the basis of the seven plant

Table 1. Mixed-effects models for effects of site, tree species richness (logSR), year, and interactions on stand-level tree basal area and volume and their increments. Fixed effects were fitted sequentially (type-I sum of squares) as indicated in the table [random terms are provided in (*24*)]. *n*, numbers of plots; df, numerator degrees of freedom; ddf, denominator degrees of freedom; and logSR, $\log_2$(tree species richness). F and *P* indicate F ratios and the *P* value of the significance test, respectively.

	Basal area (*n* = 387)				Volume (*n* = 387)				Basal area increment (*n* = 387)				Volume increment (*n* = 387)			
Source of variation	df	ddf	F	*P*	df	ddf	F	*P*	df	ddf	F	*P*	df	ddf	F	*P*
Site	1	120.0	14.35	<0.001	1	100.0	20.79	<0.001	1	121.5	8.12	0.005	1	101.3	20.79	<0.001
LogSR	1	111.9	7.45	0.007	1	88.9	6.62	0.012	1	113.8	15.58	<0.001	1	91.2	12.41	<0.001
Year	4	489.4	309.0	<0.001	4	402.3	197.10	<0.001	3	287.5	9.90	<0.001	3	281.8	35.05	<0.001
Site × year	4	488.3	7.75	<0.001	4	410.4	20.92	<0.001	3	301.0	9.43	<0.001	3	309.0	19.62	<0.001
LogSR × year	4	456.2	15.21	<0.001	4	368.9	11.98	<0.001	3	265.6	3.82	0.010	3	259.0	6.18	<0.001

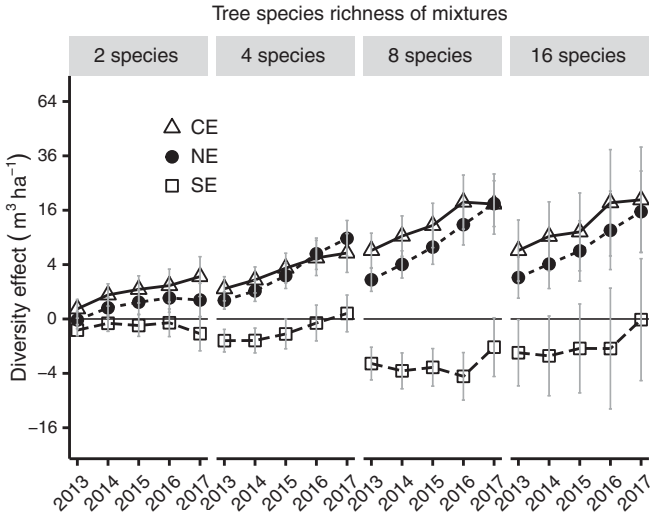

Fig. 2. Changes over time in the net biodiversity effect (NE) and its additive components, complementarity effect (CE) and selection effect (SE), on stand-level tree volume in mixed-species plots. *N* = 65 to 77, 50 to 52, 28, and 14 plots for two-, four-, eight-, and 16-species mixtures, respectively. The figure shows means ± SEs. The *y* axis is square root–scaled to reflect the quadratic nature of biodiversity effects (*10*).

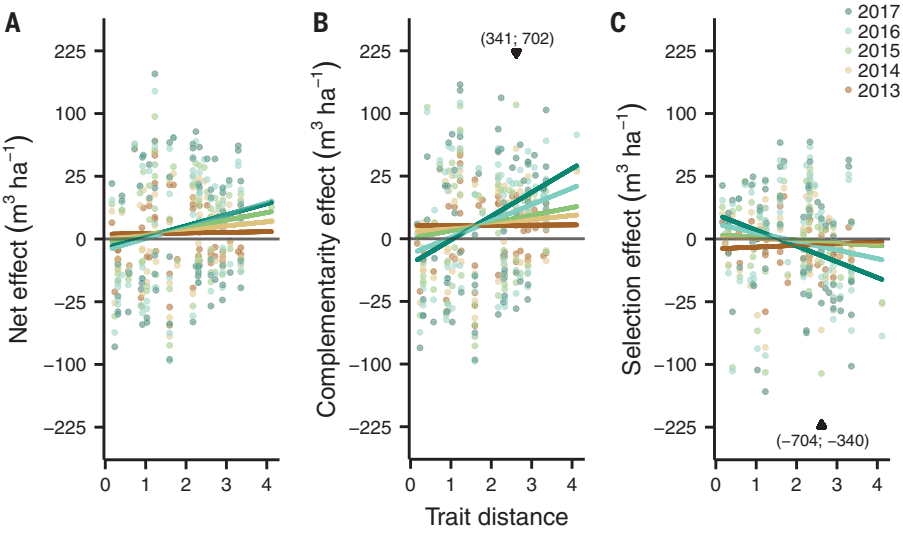

Fig. 3. Relationship between functional trait distance and biodiversity effects on stand volume in two-species mixtures across years. (**A** to **C**) Each point represents a plot in a year (*n* = 65 to 77 plots). Regression lines are based on mixed-effects models (*24*). Euclidean trait distances were calculated with the three *z*-transformed traits LD, SLA, and WD. The *y* axes are square root–scaled to reflect the quadratic nature of biodiversity effects (*10*). Two extreme *y* values are moved to the plot margin and given as numbers.

functional traits LD (deciduous or evergreen), SLA, WD, leaf dry matter content, leaf nitrogen, leaf phosphorus, and leaf thickness or the first three of these (LD, SLA, and WD), which contributed most to explanatory power. We also calculated phylogenetic diversity (PD) and mean phylogenetic distance (MPD) for each community (*24*). All measures of functional and phylogenetic diversity had similar explanatory power as that of species richness for stand-level productivity measures; differences between species-richness levels in stand volume could also be explained by associated differences in functional or phylogenetic diversity (fitted before species richness in model 1 in tables S3 and S4, respectively). However, none of the functional or phylogenetic diversity measures could explain additional variation among communities of the same richness level (when fitted after species richness in model 2 in tables S3 and S4, respectively). This finding is consistent with similar reports from large-scale grassland biodiversity experiments (*28*). It is conceivable that for each particular species mixture with high stand-level productivity, a particular combination of functional traits causes the observed biodiversity effect; this cannot be captured by using the same functional diversity measure for all species mixtures.

Earlier studies have suggested that positive biodiversity effects in forests might originate from denser crown packing and enhanced light interception in mixed-species canopies (*21*, *29*, *30*). We measured the vertical crown extent of all trees in 2016 and 2017 and tested whether plots with less crown overlap produced greater stand-level volume (*24*), which was not the case ($F_{1,446.8}$ = 1.73, P = 0.189). A reason for the absence of such a correlation might be that depending on the particular species combination, crown dissimilarity can result from light competition (*18*) or from complementary light use among species.

Despite the absence of general effects of functional diversity beyond species richness, we found some specific effects along the multiple extinction scenarios inherent in our experimental design (fig. S2A) (*24*). Changes in FD with each halving of species richness were negatively correlated with stand-volume changes at high but positively correlated at low species richness (fig. S8A), suggesting that FD captured beneficial differences between species at low but not at high diversity. We then focused on mixtures of two species because for these, the highest number of distinct species compositions were available. We found that a positive correlation of net biodiversity and complementarity effects with functional-trait distances developed over the 5 years of measurements (Fig. 3 and table S5). This was also the case for the diversity of the trait LD, indicating that mixtures of a shade-tolerant evergreen and a shade-intolerant deciduous broad-leaved species captured more light than did species pairs with uniform leaf duration.

Extinction sequences that differed in trajectories of community-weighted means for LD, SLA, or WD (fig. S2, B to D) did not show any significant variation in species-richness effects on stand-level productivity (fig. S8, B to D). This suggests that effects of trait-based extinctions, at least the ones tested and often considered most important (*25*, *26*), may not differ much from effects of random extinction. Different results might have been obtained with other trait-based extinction scenarios, either ones that we did not analyze (for example, based on root traits) or ones that we did not simulate.

Plots additionally planted with shrubs (*24*) had reduced stand-level tree volume ($F_{1,234.5}$ = 7.30, P = 0.007), which is consistent with other findings that shrub removal in forests can increase tree growth (*31*). However, the effect of shrub competition decreased with increasing shrub species richness (log shrub richness $F_{1,191.9}$ = 6.57, P = 0.011), even though stand-level basal area of shrubs did not decrease (fig. S9). The reduced competition between shrubs and trees at higher shrub diversity suggests that complementarity effects extend to tree interactions with shrubs.

Our results provide strong evidence for a positive effect of tree species richness on tree productivity at stand level in establishing subtropical forest ecosystems and support the idea that cooccurring species in highly diverse subtropical forest can differ in niches and competitive abilities. At the end of the observation period, mixed stands with 16 species had accumulated about 1.7 times the amount of C found in the average monoculture (fig. S5). This effect is, on a relative scale, similar to the 1.8-fold average increase in aboveground stand biomass from monocultures to 16-species mixtures in a multisite grassland biodiversity experiment (*4*). Given that plant biomass is higher in forests, and that the largest

fraction of tree C is bound in relatively persistent woody biomass, these effects translate into large diversity-mediated rates of C accumulation. Specifically, after 8 years of growth at site A, we found an extra 19.5 (95% CI, 14.1 to 25.1) Mg C ha^{-1} accumulated in 16-species mixtures relative to the average monoculture. The biodiversity-productivity effects that we found did not differ between 1-mu and 4-mu plots ($F_{1,118.5}$ = 0.07, P > 0.5 for interaction log tree species richness × plot size). However, biodiversity effects might be even larger at spatial scales beyond the ones that we tested experimentally because environmental heterogeneity might promote spatial insurance effects (*32*). Our first-order extrapolation to the global scale indicated that a 10% decrease in tree species richness would lead to a 2.7% decrease in forest productivity on average (*24*), which is within the range of productivity decreases (2.1 to 3.1%) reported for the same tree species loss scenario in a recent observational study that used plot data covering a large part of the global forests (*3*). In that study, it was estimated that such a loss would correspond to around $20 billion per year of commercial wood production.

Substantial forest areas are managed worldwide, with large afforestation programs underway (*33*, *34*); in China, the total forested area increased by 1.5 × 10^6 ha $year^{-1}$ from 2010 to 2015, mainly because of new monoculture plantation of species with high short-term productivity (*35*). Our experimental findings suggest that a similar or potentially even higher productivity can be achieved with mixed plantations of native species. Such strategies would yield cobenefits (*2*) in terms of active biodiversity management and likely higher levels of stability of productivity and ecosystem services under adverse conditions such as pathogen infestation or future climate change, including extreme events.

REFERENCES AND NOTES

1. A. S. Mori, *J. Ecol.* **106**, 113–125 (2018).
2. L. Gamfeldt *et al*., *Nat. Commun.* **4**, 1340 (2013).
3. J. Liang *et al*., *Science* **354**, eaaf8957 (2016).
4. A. Hector *et al*., *Science* **286**, 1123–1127 (1999).
5. P. B. Reich *et al*., *Science* **336**, 589–592 (2012).
6. D. Tilman, D. Wedin, J. Knops, *Nature* **379**, 718–720 (1996).
7. D. Tilman, C. L. Lehman, K. T. Thomson, *Proc. Natl. Acad. Sci. U.S.A.* **94**, 1857–1861 (1997).
8. S. A. Schnitzer *et al*., *Ecology* **92**, 296–303 (2011).
9. M. A. Huston, *Oecologia* **110**, 449–460 (1997).
10. M. Loreau, A. Hector, *Nature* **412**, 72–76 (2001).
11. H. Bruelheide *et al*., *Ecol. Monogr.* **81**, 25–41 (2011).
12. S. P. Hubbell, *Ecology* **87**, 1387–1398 (2006).
13. X. Wang *et al*., *Ecology* **97**, 347–360 (2016).
14. M. Scherer-Lorenzen, "The functional role of biodiversity in the context of global change" in *Forests and Global Change*, D. A. Coomes, D. F. R. P. Burslem, W. D. Simonson, Eds. (Cambridge Univ. Press, 2014), pp. 195–238.
15. K. Verheyen *et al*., *Ambio* **45**, 29–41 (2016).
16. J. J. Grossman, J. Cavender-Bares, S. E. Hobbie, P. B. Reich, R. A. Montgomery, *Ecology* **98**, 2601–2614 (2017).
17. C. Potvin, N. J. Gotelli, *Ecol. Lett.* **11**, 217–223 (2008).
18. J. Sapijanskas, A. Paquette, C. Potvin, N. Kunert, M. Loreau, *Ecology* **95**, 2479–2492 (2014).
19. C. M. Tobner *et al*., *Ecol. Lett.* **19**, 638–647 (2016).
20. T. Van de Peer, K. Verheyen, Q. Ponette, N. N. Setiawan, B. Muys, *J. Ecol.* **106**, 1096–1105 (2017).
21. L. J. Williams, A. Paquette, J. Cavender-Bares, C. Messier, P. B. Reich, *Nat. Ecol. Evol.* **1**, 63 (2017).
22. D. A. Clarke, P. H. York, M. A. Rasheed, T. D. Northfield, *Trends Ecol. Evol.* **32**, 320–323 (2017).
23. H. Bruelheide *et al*., *Methods Ecol. Evol.* **5**, 74–89 (2014).
24. Materials and methods are available as supplementary materials.
25. P. B. Adler, A. Fajardo, A. R. Kleinhesselink, N. J. B. Kraft, *Ecol. Lett.* **16**, 1294–1306 (2013).
26. S. Greenwood *et al*., *Ecol. Lett.* **20**, 539–553 (2017).
27. E. Marquard *et al*., *J. Ecol.* **97**, 696–704 (2009).
28. D. F. B. Flynn, N. Mirotchnick, M. Jain, M. I. Palmer, S. Naeem, *Ecology* **92**, 1573–1581 (2011).
29. T. Jucker, O. Bouriaud, D. A. Coomes, *Funct. Ecol.* **29**, 1078–1086 (2015).
30. P. A. Niklaus, M. Baruffol, J.-S. He, K. Ma, B. Schmid, *Ecology* **98**, 1104–1116 (2017).
31. R. G. Wagner, K. M. Little, B. Richardson, K. McNabb, *Forestry* **79**, 57–79 (2006).
32. F. Isbell *et al*., *Nature* **546**, 65–72 (2017).
33. Food and Agriculture Organization of the United Nations (FAO), *Global Forest Resources Assessment* (FAO, 2015).
34. R. J. Keenan *et al*., *For. Ecol. Manage.* **352**, 9–20 (2015).
35. F. Hua *et al*., *Nat. Commun.* **7**, 12717 (2016).

ACKNOWLEDGMENTS

We thank farmers for help in the field. **Funding:** This study was supported by the German Research Foundation (DFG FOR 891), the Strategic Priority Research Program of the Chinese Academy of Sciences (nos. XDB31000000 and XDA19050000), the National Natural Science Foundation of China (NSFC nos. 31270496 and 31300353), the Swiss National Science Foundation (SNSF nos. 130720 and 147092), and the European Union (EC 7th Framework Program no. 608422). **Author contributions:** Y.H. and Y.C. are co-first authors. H.B., W.H., J.-S. H., A.H., K.M., T.S., and B.S. conceived the project; M.Ba., M.Br., N.C., D.E., J.F., Y.H., Y.L., S.L., X.L., S.M., T.S., X.Y., and B.Y. collected the data; Y.H., Y.C., P.A.N., and B.S. analyzed and interpreted the data and wrote the manuscript. All authors discussed the results and contributed to the final manuscript. **Competing interests:** The authors declare no competing interests. **Data and materials availability:** The data supporting the findings of this study are deposited in Dryad with the accession code doi: 10.5061/dryad.t86145r.

SUPPLEMENTARY MATERIALS

www.sciencemag.org/content/362/6410/80/suppl/DC1
Materials and Methods
Supplementary Text
Figs. S1 to S9
Tables S1 to S5
References (*36*–*57*)

2 May 2018; accepted 24 August 2018
10.1126/science.aat6405

Science

Impacts of species richness on productivity in a large-scale subtropical forest experiment

Yuanyuan Huang, Yuxin Chen, Nadia Castro-Izaguirre, Martin Baruffol, Matteo Brezzi, Anne Lang, Ying Li, Werner Härdtle, Goddert von Oheimb, Xuefei Yang, Xiaojuan Liu, Kequan Pei, Sabine Both, Bo Yang, David Eichenberg, Thorsten Assmann, Jürgen Bauhus, Thorsten Behrens, François Buscot, Xiao-Yong Chen, Douglas Chesters, Bing-Yang Ding, Walter Durka, Alexandra Erfmeier, Jingyun Fang, Markus Fischer, Liang-Dong Guo, Dali Guo, Jessica L. M. Gutknecht, Jin-Sheng He, Chun-Ling He, Andy Hector, Lydia Hönig, Ren-Yong Hu, Alexandra-Maria Klein, Peter Kühn, Yu Liang, Shan Li, Stefan Michalski, Michael Scherer-Lorenzen, Karsten Schmidt, Thomas Scholten, Andreas Schuldt, Xuezheng Shi, Man-Zhi Tan, Zhiyao Tang, Stefan Trogisch, Zhengwen Wang, Erik Welk, Christian Wirth, Tesfaye Wubet, Wenhua Xiang, Mingjian Yu, Xiao-Dong Yu, Jiayong Zhang, Shouren Zhang, Naili Zhang, Hong-Zhang Zhou, Chao-Dong Zhu, Li Zhu, Helge Bruelheide, Keping Ma, Pascal A. Niklaus and Bernhard Schmid

Science **362** (6410), 80-83.
DOI: 10.1126/science.aat6405

Tree diversity improves forest productivity

Experimental studies in grasslands have shown that the loss of species has negative consequences for ecosystem functioning. Is the same true for forests? Huang *et al.* report the first results from a large biodiversity experiment in a subtropical forest in China. The study combines many replicates, realistic tree densities, and large plot sizes with a wide range of species richness levels. After 8 years of the experiment, the findings suggest strong positive effects of tree diversity on forest productivity and carbon accumulation. Thus, changing from monocultures to more mixed forests could benefit both restoration of biodiversity and mitigation of climate change.

Science, this issue p. 80

www.sciencemag.org/content/362/6410/80/suppl/DC1

Supplementary Material for

Impacts of species richness on productivity in a large-scale subtropical forest experiment

Yuanyuan Huang, Yuxin Chen, Nadia Castro-Izaguirre, Martin Baruffol, Matteo Brezzi, Anne Lang, Ying Li, Werner Härdtle, Goddert von Oheimb, Xuefei Yang, Xiaojuan Liu, Kequan Pei, Sabine Both, Bo Yang, David Eichenberg, Thorsten Assmann, Jürgen Bauhus, Thorsten Behrens, François Buscot, Xiao-Yong Chen, Douglas Chesters, Bing-Yang Ding, Walter Durka, Alexandra Erfmeier, Jingyun Fang, Markus Fischer, Liang-Dong Guo, Dali Guo, Jessica L. M. Gutknecht, Jin-Sheng He, Chun-Ling He, Andy Hector, Lydia Hönig, Ren-Yong Hu, Alexandra-Maria Klein, Peter Kühn, Yu Liang, Shan Li, Stefan Michalski, Michael Scherer-Lorenzen, Karsten Schmidt, Thomas Scholten, Andreas Schuldt, Xuezheng Shi, Man-Zhi Tan, Zhiyao Tang, Stefan Trogisch, Zhengwen Wang, Erik Welk, Christian Wirth, Tesfaye Wubet, Wenhua Xiang, Mingjian Yu, Xiao-Dong Yu, Jiayong Zhang, Shouren Zhang, Naili Zhang, Hong-Zhang Zhou, Chao-Dong Zhu, Li Zhu, Helge Bruelheide*, Keping Ma*, Pascal A. Niklaus*, Bernhard Schmid*

‡Corresponding author. Email: helge.bruelheide@botanik.uni-halle.de (H.B.); kpma@ibcas.ac.cn (K.M.); pascal.niklaus@ieu.uzh.ch (P.A.N.); bernhard.schmid@ieu.uzh.ch (B.S.)

Published 5 October 2018, *Science* **362**, 80 (2017)
DOI: 10.1126/science.aat6405

This PDF file includes:

Materials and Methods

Study site and experimental design

The BEF-China experimental platform is located in Jiangxi Province, China (29°08′–29°11′N, 117°90′–117°93′E). Climate at the site is subtropical, with mean annual temperature and precipitation of 16.7 °C and 1800 mm, respectively (averaged from 1971–2000) (*36*). During the study period from 2013–2017 mean annual temperature was 18.1, 18.0, 17.5, 18.0 and 17.9 °C, whereas annual precipitation was more variable with 1354, 2110, 2632, 1944 and 2338 mm, respectively *(37)*. The region is covered by subtropical broad-leaved forest and plantations of two commercially important coniferous species, *Pinus massoniana* and *Cunninghamia lanceolata* (see below). We established a large-scale tree biodiversity experiment in 2009–2010 at two sites (A and B) of approximately 20 ha each. These sites were previously used as *Cunninghamia lanceolata* plantations, which still surround the experimental sites. We planted a total of 226,400 individual trees on 566 plots *(23)*. For the present study we used 396 plots, planted with a total of 158,400 individuals, in which species-loss scenarios were simulated that included each of 40 species at each level of species richness from 24 to sixteen, eight, four, two and one species and the two conifers as reference monocultures. Species names and abbreviations together with major characteristics and initial size at planting are provided in Table S1.

Three pools of 16 species were created at each site: A1–A3 and B1–B3 (Tables S1 and S2). The species in each 16-species pool were put in random sequence and then repeatedly divided in halves until monocultures were obtained. For each site, this procedure resulted in 69 unique species compositions plus one 24-species mixture combining all species of the three pools of that site plus the reference monocultures of the two conifers. Each plot was 25.8 × 25.8 m in size (Chinese area unit of 1 mu) and planted with 400 tree individuals arranged in a rectangular 20 × 20 grid with 1.29 m spacing between rows and columns, corresponding to an area of 1.675 m^2 per individual at planting. Planting density for species such as *Cunninghamia lanceolata* in commercial plantations around the field site is 1 tree per 4 m^2 (2 m distance between trees). Accounting for mortality, which on average was 6 out of 16 central trees (Fig. S6), the average area per tree had increased to about 3 m^2 by 2017. Our objective when establishing a relatively high planting density was to allow for early interactions among trees, as would be expected in natural stands at the experimental site *(11)*. From measurements at site A over the four-year period 2013–2016 we found that mean crown projection area per tree increased from 1.1–2.7 m^2 in the average monoculture and from 2.2–4.1 m^2 in the average 16-species mixture, leading to LAI values that increased from 1.1-1.8 in the average monoculture and from 1.5-3.7 in the average 16-species mixture. To minimize edge effects, plots were established adjacent to each other, with trees thus forming a continuous cover across the entire site. Site A was planted in 2009, site B in 2010.

Plots were randomly distributed in rectangular grids across the two sites (Fig. S1). Each species composition of pools A1 and B1 was replicated across five plots, of which four were arranged into a larger quadrat of 51.6 × 51.6 m. This was done to allow two additional treatment effects to be tested: plot size (1 mu vs. 4 mu) and species richness of understory shrubs. For the latter treatment the four plots in a larger quadrat were planted with 0, 2, 4 or 8 shrub species, randomly selected from a pool of 18 species, at the same total density as the trees; each individual shrub was planted in the center between four adjacent trees. Species compositions of pools A2, A3, B2 and B3 were planted in only one plot each and without shrub addition. Of the 396 plots, nine had to be excluded because these were not established due to a lack of sapling material or high initial mortality. All plots were weeded annually to remove emerging herbs and woody species that were not part of the planting design.

Tree measurements

We studied how changing tree species richness along the different functional-trait trajectories of simulated extinction scenarios in BEF-China affected the stand-level development of tree basal area, aboveground volume and aboveground carbon from 2013–2017. These productivity-related variables were derived from direct measurements of tree basal diameter and height, using allometric equations determined by complete aboveground harvests of young trees in a forest near the experimental area. The direct measurements were taken for all survivors of the 16 central trees in each plot of 400 trees in September/October within at most 23 consecutive days per site per year. Because we analyzed plot-level rather than individual-level data, we focused on a comparatively large number of replicates at plot rather than individual level within the given time available for measurements. A larger number of trees sampled within plots would have increased the precision of the plot-level data and the chances to obtain higher significance levels for treatment effects.

Data from 154 separately harvested trees near the experimental site were used to obtain conversion factors to calculate aboveground tree volume and biomass from the direct measurements of basal diameter and height (see section "Conversion factors for individual tree volume and biomass" below) and aggregated the individual data to the stand level. Biomass was converted to carbon content (*38*) by multiplying with 0.474 g C g^{-1}. To characterize annual stand growth, we further derived yearly increments of stand basal area, stand volume and stand carbon from successive inventories. We determined the same metrics at the population level (stand-level data separated into species). We used a Bayesian approach to estimate the uncertainties of plot-level carbon arising from the use of different allometric equations for experimental species and the two commercial monoculture species (see section "Estimation of aboveground carbon and its uncertainties" below).

Conversion factors for individual tree volume and biomass

We harvested 154 trees in a natural forest in 2010 near the experimental sites to determine conversion factors from cylindrical volume (tree basal area × height) to true volume and biomass (*39*). The trees belonged to eight common species and three life forms (evergreen angiosperms, deciduous angiosperms and conifers) and were chosen to represent a naturally occurring size span of young trees.

Trees were separated into large woody parts (stems and large branches with a diameter ≥ 3 cm), twigs (the apical part of the stem and large branches plus side branches with a diameter < 3 cm) and dead attached material (large dead branches or twigs). Branches were divided into segments of about 1 m length. The volume of large woody parts and twigs was determined geometrically, approximating the parts as truncated cones (large woody parts, $V = \frac{1}{3}\pi (r_1^2+r_1 r_2+r_2^2) L$ where L is the length and r_1 and r_2 are the end radii), or cones (twigs, as above but $r_2 = 0$). The density of these fractions was determined by oven-drying a representative subsample of stem and branch discs or twigs. These geometric and density data were then scaled up to total aboveground tree biomass, modeling twig mass and density in dependence of branch positions within tree crowns (*39*).

Conversion factors from cylindrical volume to true volume (and mass) were determined as total tree volume (and tree mass, including leaves) divided by cylindrical volume. We analyzed the variation of these conversion factors with tree size and species life form using mixed-effects models with species identity as random term. We found that large trees deviated from the linear relationship between form factor and cylindrical volume, and we therefore removed trees with a

cylindrical volume ≥ 0.5 m^3 from the calibration, leaving a set of 119 trees. Within this set, there was only a small variance among species and no significant effect of life form on the form factor; the form factor decreased linearly with the cylindrical volume of harvested trees. We therefore used a form factor of 0.5412 $m^3\ m^{-3}$−0.1985 m^{-3} BA h (with basal area BA in m^2 and height h in m). The intercept of 0.5412 $m^3\ m^{-3}$ is the weighted average form factor of evergreen and deciduous species at size zero (in our study, 19 of 40 species were evergreen and 21 deciduous). Biomass factors were determined similarly, yielding a conversion factor of 269.13 kg m^{-3}−141.96 kg m^{-6} BA h. For the two coniferous species, *Pinus massoniana* and *Cunninghamia lanceolata*, we used separate equations obtained from the harvested trees of these two species. Here the form factor was 0.5083 $m^3\ m^{-3}$−0.1985 m^{-6} BA h and the biomass factor was 216.79 kg m^{-3}−141.96 kg m^{-6} BA h.

Using the conversion factors obtained from the harvested trees in allometric equations we estimated their volume and biomass from basal area and height; the estimated volume was strongly correlated with the real volume of the trees (r^2 = 0.907 for angiosperms and r^2 = 0.891 for gymnosperms) and the same was the case for estimated and real biomass (r^2 = 0.913 for angiosperms and r^2 = 0.830 for gymnosperms).

Estimation of aboveground carbon and its uncertainties

We used Bayesian statistical techniques to estimate plot-level carbon after eight years of growth (site A in 2017) and its uncertainty arising from the allometry models. First, we re-fitted the allometric models with the data of harvested trees as we did in the non-Bayesian approach:

$$y_{i,j,k} \sim N\left(\alpha_k + \beta\ rv_{i,j,k} + \gamma_j, \sigma\right) \quad (S1),$$

where $y_{i,j,k}$ is the conversion factor for biomass derived from harvested tree *i* of species *j* and life form *k*; $rv_{i,j,k}$ is the raw volume of harvested trees calculated as cylindrical volume, α_k is life-form specific intercept, β is the slope, γ_j is the species-level random effect and σ is the model error. The Bayesian models produced similar results as those from non-Bayesian methods using linear mixed-effects models.

Then we used the fitted Bayesian allometric models (eqn. S1) to predict the posterior distribution of the conversion factors for each tree in the main experiment:

$$\hat{y}_t \sim N(\bar{\alpha} + \beta\ rv_t, \sigma) \quad (S2),$$

where $\hat{y}_t$ is the predicted conversion factor for biomass of tree *t* from the main experiment, $\bar{\alpha}$ is the average intercept weighted by the proportion of the corresponding life form in the experiment and rv_t is the raw volume of tree *t*. We omitted species-level random effects in equation S2 because we found only a small variance among species. The posterior distribution of biomass was derived as $\hat{y}_t \times rv_t$. We further derived the posterior distribution of carbon as the product of predicted biomass and carbon density. Finally, we calculated the posterior distribution of plot-level carbon by summing the tree-specific carbon values within each plot. Therefore, the plot-level carbon contained the uncertainties from both the allometric parameters ($\bar{\alpha}$ and β) and model error (σ).

We fitted equations S1 and S2 together in a single Bayesian model. We ran the Bayesian models in JAGS 4.2.0 using the rjags package (*40*) with three parallel chains. We set diffuse priors for each parameter and assessed the parameter convergence with Gelman and Rubin's convergence diagnostics (with a threshold value < 1.05) (*41*).

Additive partitioning of net biodiversity effects into complementarity and selection effects

We used the additive partitioning method of Loreau and Hector (*10*) to decompose net biodiversity effects (NEs) of productivity measures into complementarity effects (CEs) and selection effects (SEs), separately for each year and diversity level. CEs and SEs depend on relative

yields of species, which we calculated using monoculture volume as denominator *(10)*. This method has the problem that very small monoculture values lead to unrealistically large relative yield values and these values should therefore be excluded from additive partitioning calculations *(42)*. We used a stand-level tree volume of 0.2 m^3 ha^{-1} in monoculture as cut-off point to avoid extreme relative yield values. Formally, CEs and SEs are related to (co-)variances and therefore were square-root transformed with sign reconstruction ($\text{sign}(y)\sqrt{|y|}$) prior to analysis, which improved the normality of residuals (*10*).

We used the following equation to calculate individual species SEs:

$$SE_i = (\Delta RY_i - \Delta\overline{RY}) \times \left(M_i - \overline{M}\right)$$

Here ΔRY_i is the deviation from expected relative yield of species i in the mixture and M_i is the yield of species i in monoculture.

Functional and phylogenetic diversity measures

We used seven functional traits to calculate measures of functional diversity for all communities in the experiment. These traits were determined in plots that were part of the experiment (*43*): leaf duration (LD, deciduous or evergreen), specific leaf area (SLA), branch-wood density (WD), leaf dry matter content, leaf nitrogen, leaf phosphorus and leaf thickness. We used species means to calculate functional diversity (FD) (*44*) and functional dispersion (FDis) (*45*). After testing the predictive power of these functional diversity measures in explaining variation in stand-level productivity measures for all traits individually and in different combinations, we retained those combining all seven traits or combining the three traits LD, SLA and WD. These three functional traits are known to be associated with a trade-off between rapid resource acquisition and fast growth vs. high tolerance to environmental stress and slower growth (*46, 47*). For these three traits we further calculated individual and multivariate Euclidean trait distance (TD) in two-species mixtures to assess its relationship with the net biodiversity effect and its components (NE, CE and SE). For the multivariate TD the three traits were first standardized with a z-transformation. We calculated two phylogenetic diversity measures (*48*) with a node age-calibrated phylogenetic tree (*49*): Faith's phylogenetic diversity (PD) and mean pairwise phylogenetic distance (MPD). FD and PD are dependent on species richness and thus encompass functional and phylogenetic diversity both among and within species-richness levels. Distance measures (FDis, TD and MPD) are independent of species richness (*48*).

Vertical crown extent and overlap

In 2016 and 2017 we measured the crown extent of each surviving tree as interval between the lowest side branch and the top of the tree. Species means per plot were then used to calculate vertical crown overlap between species as proportional similarity *(30)*, $PS_{A,B} = A \cap B / A \cup B$, where $A \cap B$ is the vertical extent that is occupied by both species and $A \cup B$ is the extent occupied by at least one of the two species A or B. For mixtures with more than two species we used the mean proportional similarity between all possible pairs as measure for vertical crown overlap.

Functional-trait trajectories of extinction sequences

We derived trait-based trajectories of extinction sequences from the changes of FDs and community-weighted mean trait values of the three functional traits LD, SLA and WD across richness gradients (Fig. S2). Community-weighted means were calculated with equal weights for all planted species in a plot. For each species pool, a single 16-species mixture leads to 16 extinction trajectories ending in different monocultures.

Statistical analysis

We used analysis of variance based on type-I sum of squares in linear mixed-effects models to assess the effects of tree species richness and other explanatory variables on productivity (*50*). All analyses were done in R 3.3.2 and ASReml-R (*51*). The models included the fixed effects site, tree species richness (log_2-transformed), year (as continuous variable, i.e. linear term—followed by annual precipitation in tests for climatic effects, or as multi-level factor), the interaction log_2(tree species richness) × year, and the interaction site × year. Random effects were species composition (with a separate variance component for each site), large plot (set of four plots arranged in a quadrat for pool A1 and B1, see Table S2; with a separate variance component for each site), plot and their interactions with year. The interaction of year and site and the site-specific variance terms estimated for some random terms accounted for the fact that site B was established one year after site A and that trees at site B were therefore smaller. Model residuals were checked for normality and homogeneity of variances; these assumptions were fulfilled without transformations of dependent variables. For the analyses of shrub diversity effects, the model contained the additional fixed effects shrub presence (a two-level factor: 0 vs. 2, 4 or 8 shrub species), log_2 of shrub species richness (for shrub-species richness > 0), plot size (a two-level factor: 1 vs. 4 mu) and the interactions of all these terms with log_2(tree species richness) and with year.

To assess whether functional or phylogenetic diversity measures explained effects of species richness or additional variation in dependent variables these measures were fitted as covariates before (model 1) or after species richness (model 2) in separate analyses of variance (Tables S3 and S4). The effects of vertical crown overlap were tested in the same way but not presented in tables because they were not significant. We further focused on two-species mixtures to assess the effects of trait distances (TD) on biodiversity effects (NE, CE and SE) using linear mixed-effects models. We set site, TD, year (factor) and the interaction between TD and year as fixed effects, community composition, plot size and their interactions with year as random effects. For these analyses diversity effects were based on the tree stand volume from 2013–2017 and were square-root transformed with sign reconstruction to improve normality of model residuals. We excluded one plot with extreme values of CE and SE (absolute value > 2000) in 2017 before model fitting. However, including this extreme plot produced qualitatively similar results.

We separated FD-based extinction scenarios (Fig. S2A) into four steps by halving species richness from 16 to 8, 8 to 4 etc. and assessed the relationship between changes in FD and volume (average across years) for each step with simple linear regression. Then, we regressed the four slopes of these regressions against step, 1 referring to extinction step 2 → 1, 2 to step 4 → 2 etc. (Fig. S8A). For the other three types of functional-trait trajectories (Fig. S2, B to D) we plotted species-richness effects (average slopes across years of stand volume vs. log_2-transformed tree species richness for each extinction sequence) against changes in functional trait means (slopes of functional trait mean vs. log_2-transformed tree species richness for each extinction sequence) and tested the relationship using simple linear regression (Fig. S7, B to D).

Supplementary Text

Productivity decrease due to 10 % loss of tree species richness

Liang *et al.* (*3*) used global forest observational data to estimate the effect of 10 % loss of tree species richness on productivity (measured as volume increment). To compare the diversity effect of our experiment with the global estimate, we predicted the productivity loss under the same pressure of species loss. First, we predicted the volume increment from 2016 to 2017 at the planted species richness (1, 2, 4, 8, 16) and their corresponding 10 % lower richness levels using our fitted mixed-effects models (Table 1). Then we took the average productivity decrease due to 10 % loss of tree richness across planted richness levels. The productivity drops would be 3.0 %, 2.5 %, 2.2 %, and 1.9 % when losing on average 10 % of the species, starting from species richness 2, 4, 8 and 16, respectively. These values correspond closely to the 2.1–3.1 % drop obtained with the power function in Liang *et al*. (*3*), which they converted to a potential yearly commercial forest productivity valued at 20 billion US$.

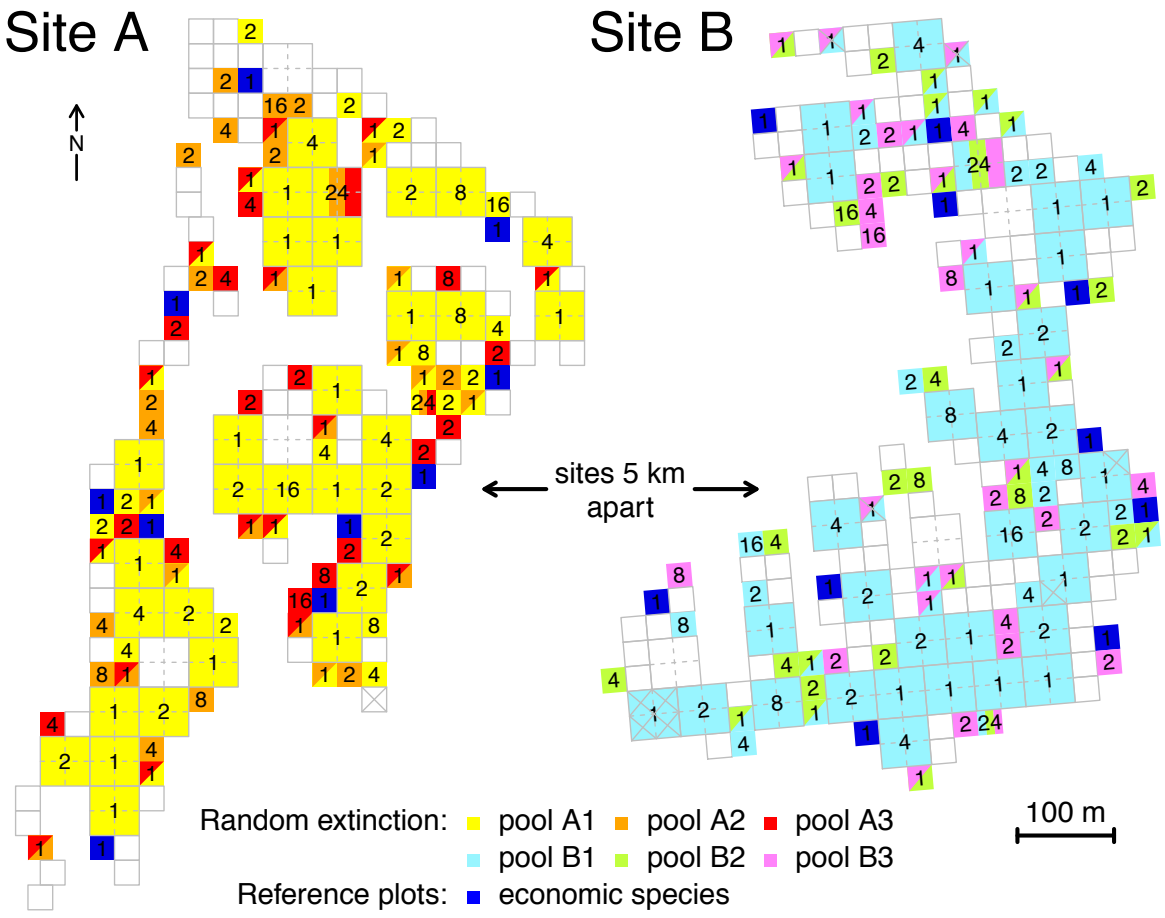

Fig. S1. Map of BEF-China experimental plots analyzed in this paper. Each species composition of pools A1 (yellow) and B1 (light blue) is replicated across five plots of which four are arranged into a larger quadrat of 51.6 × 51.6 m; species compositions of pools A2, A3, B2 and B3 (other colors) are not replicated (see Tables S1, S2). Monocultures of two commercial conifers, *Pinus massoniana* and *Cunninghamia lanceolata*, are replicated at both sites in five plots each (dark blue). Note that in some cases two pools share a monoculture species (plots with diagonal coloring). Empty plots belong to the overall BEF-China experiment but not to the treatments analyzed in the present paper.

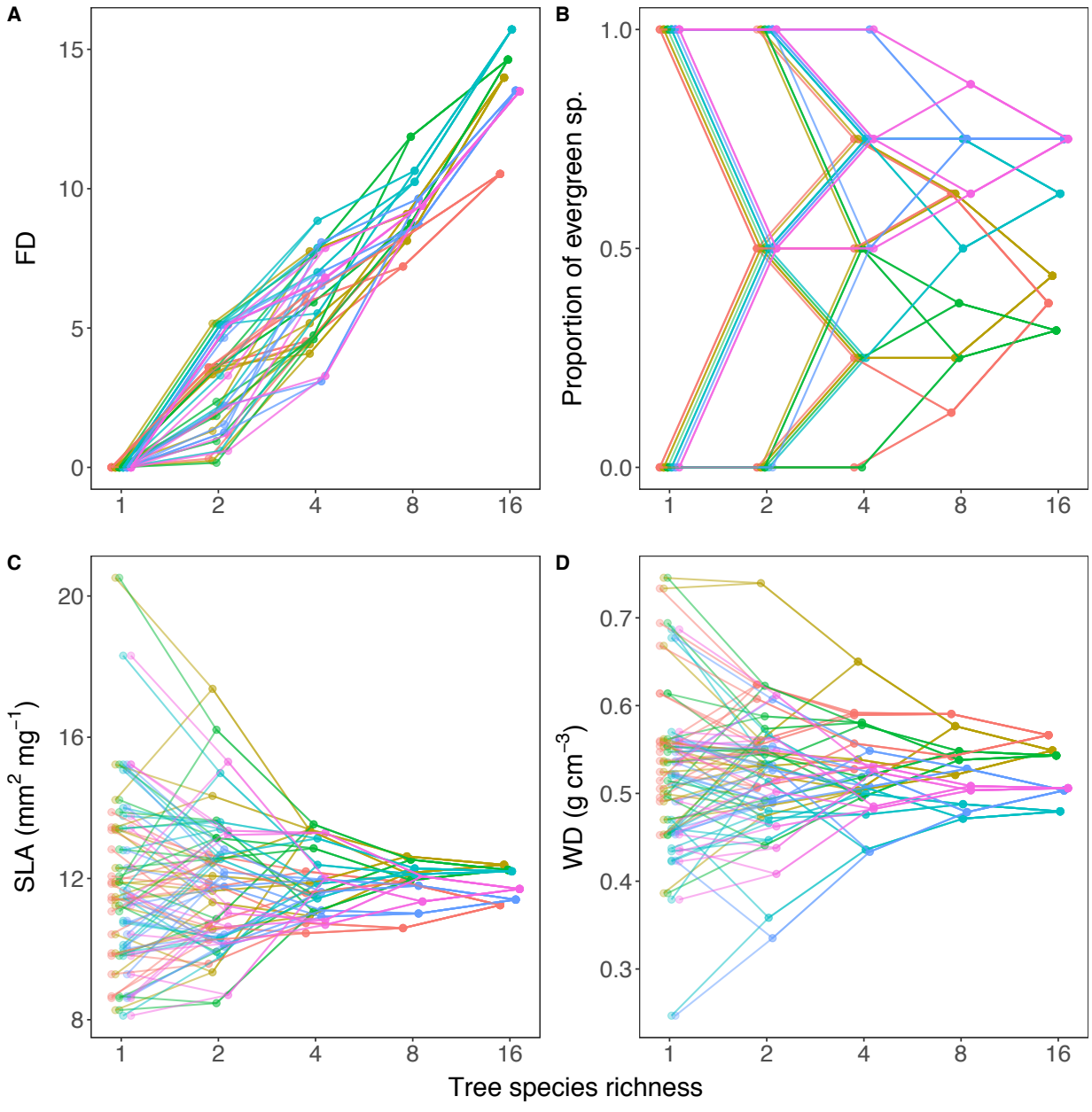

Fig. S2. Functional-trait trajectories of the different extinction sequences based on functional-trait diversity FD (A), mean leaf-duration class (proportion of evergreen species) (B), mean specific leaf area (SLA) (C) and mean wood density (D). Extinction sequences are shown from right to left as function of species richness (log_2-scale). Different colors represent different species pools. FD was calculated with the three functional traits shown in B–D. Means in B–D are community-weighted means with species weighted equally.

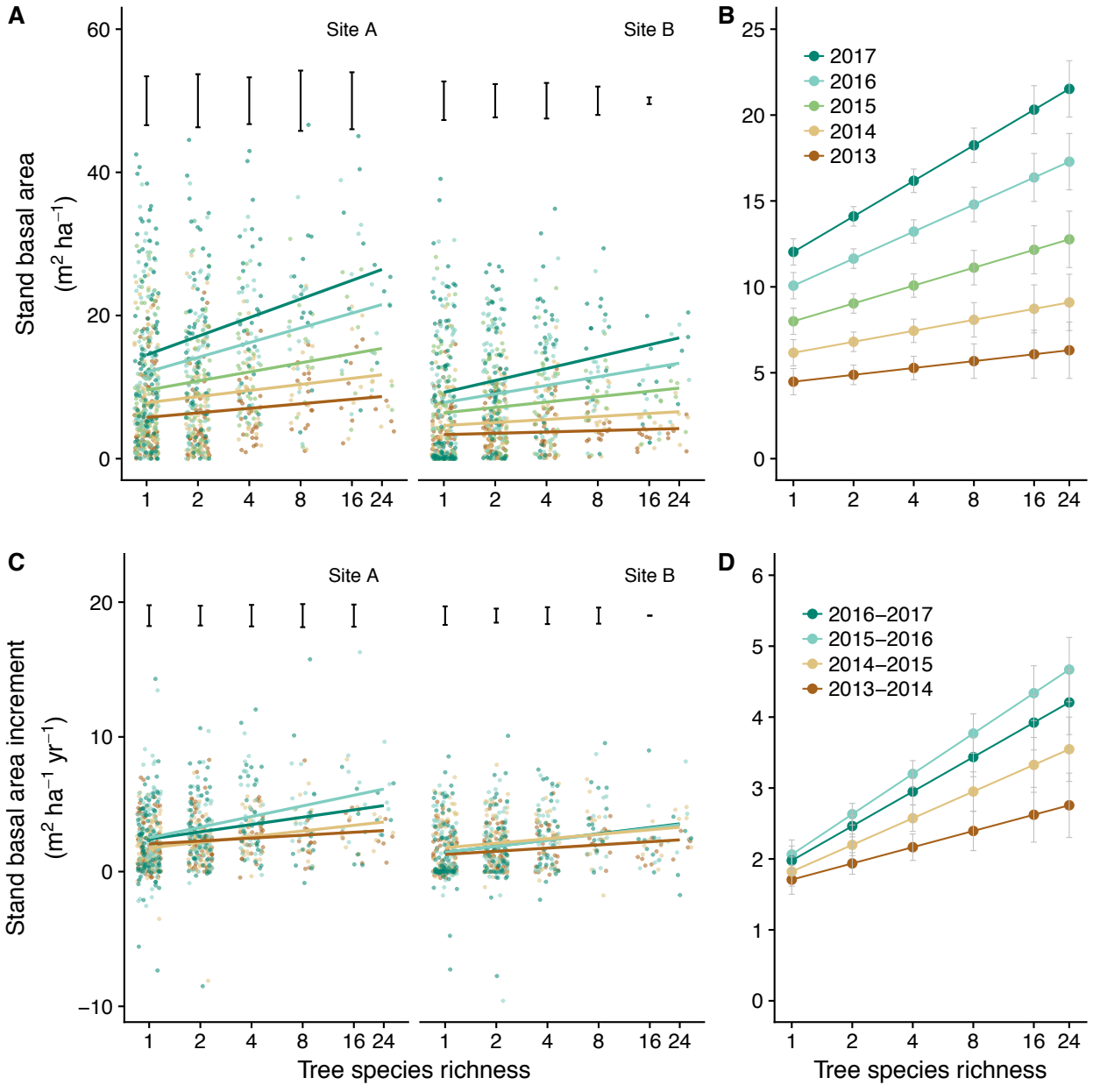

Fig. S3. Stand-level tree basal area (A, B) and its annual increment (C, D) as a function of tree species richness from 2013–2017. In panels A and C, raw data points and regression lines are shown for each year. Panels B and D show predicted means ± standard errors based on mixed models (Table 1). Standard deviations of species compositions (square root of corresponding between-composition variance components) are shown as black error bars above the raw data.

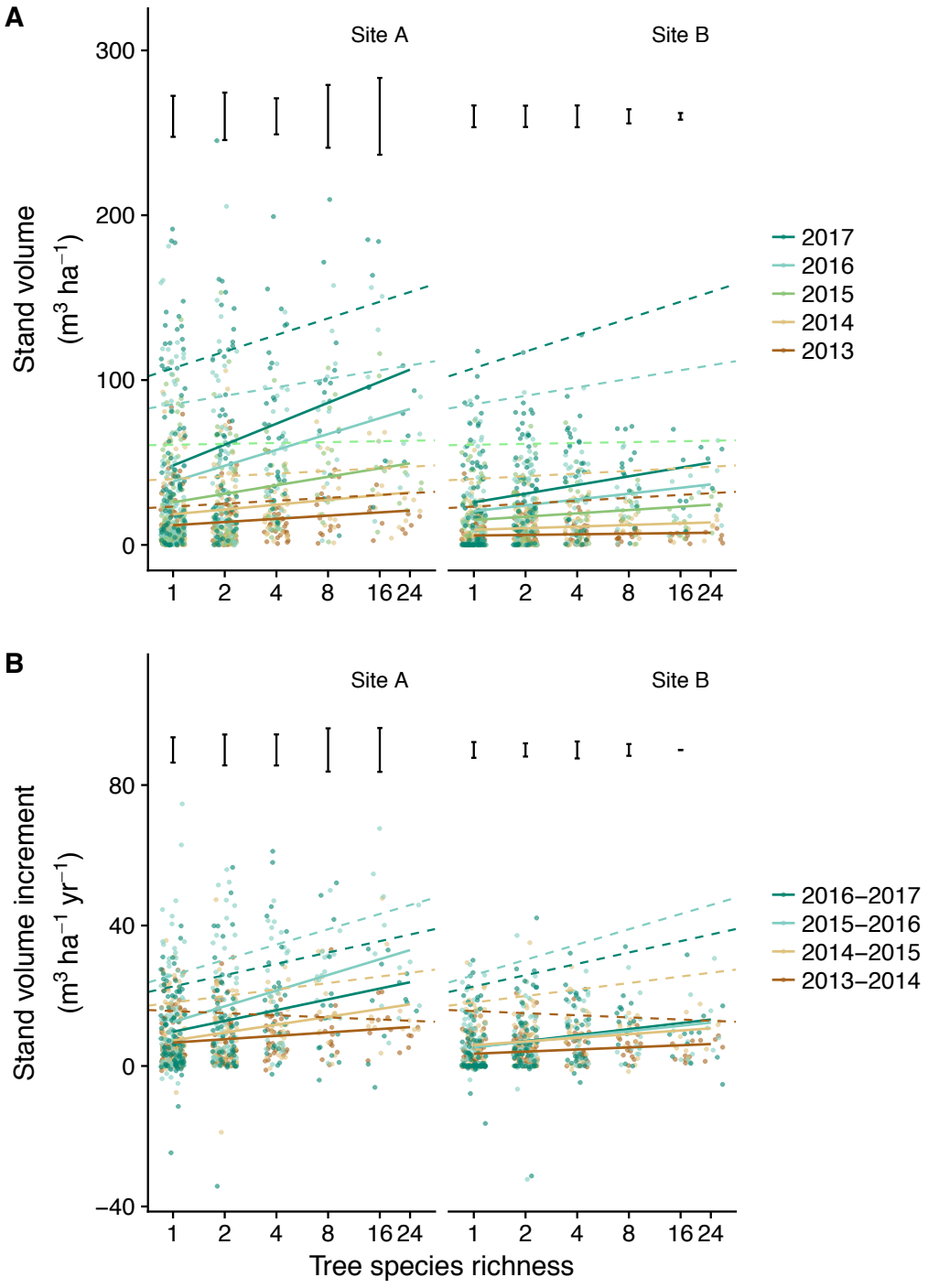

Fig. S4. Stand-level tree volume (A) and its increment (B) as a function of tree species richness from 2013–2017. The figure panels A and B correspond to panels A and C in Fig. 2 of the main text, respectively, but with dashed quantile regression lines for the largest 10% of values at each diversity level added to the solid regression lines fitted across all values for each year. Standard deviations of species compositions (square root of corresponding between-composition variance components) are shown as black error bars.

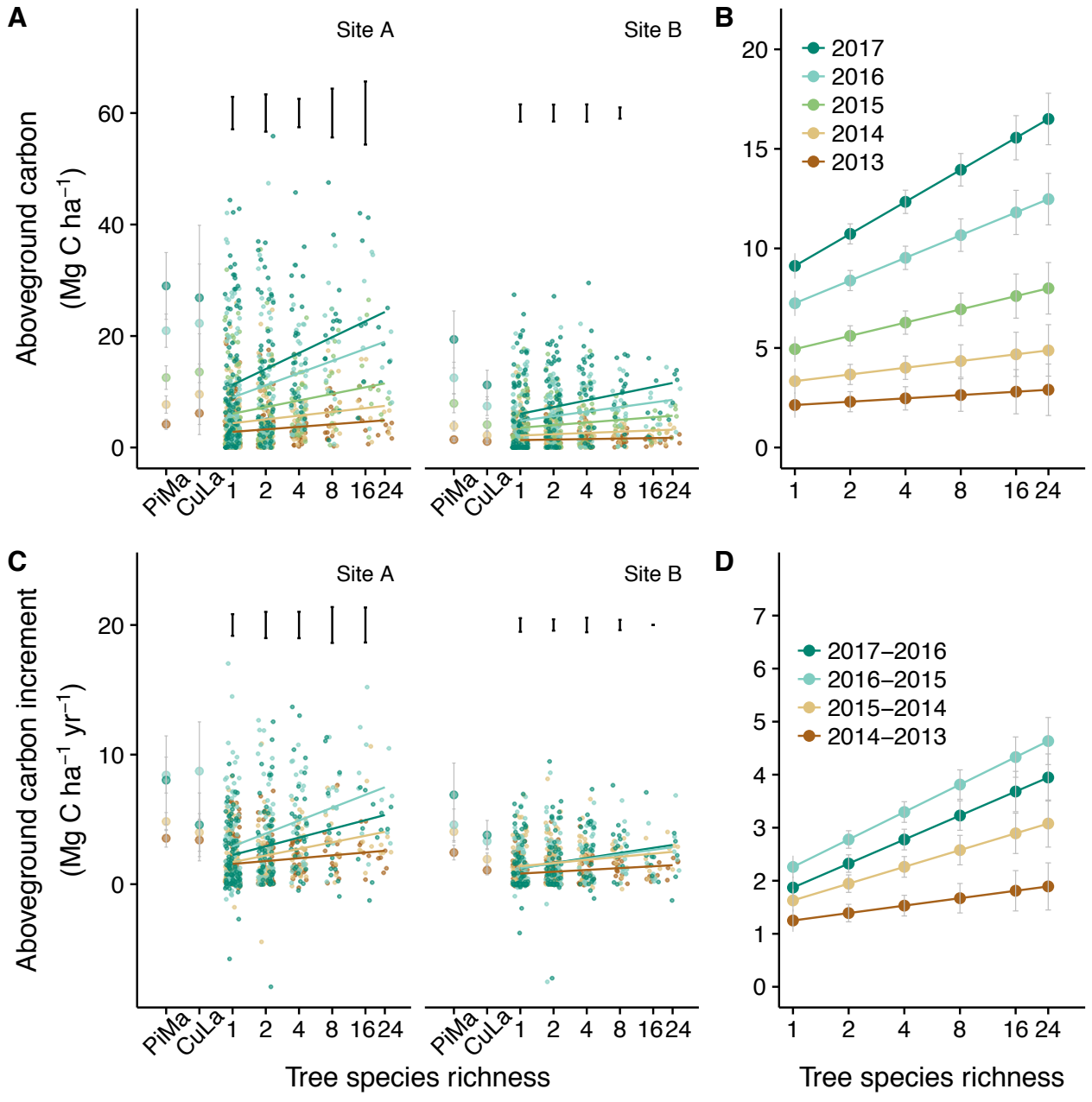

Fig. S5. Aboveground stand-level tree carbon (A, B) and its annual increment (C, D) as a function of tree species richness from 2013–2017. In panels A and C, raw data points and regression lines are shown for each year. On the left of each panel, means ± standard errors for the two economic tree species are shown (PiMa = *Pinus massoniana*; CuLa = *Cunninghamia lanceolata*). Panels B and D show predicted means ± standard errors based on mixed models (Table 1). Standard deviations of species compositions (square root of corresponding between-composition variance components) are shown as black error bars above the raw data.

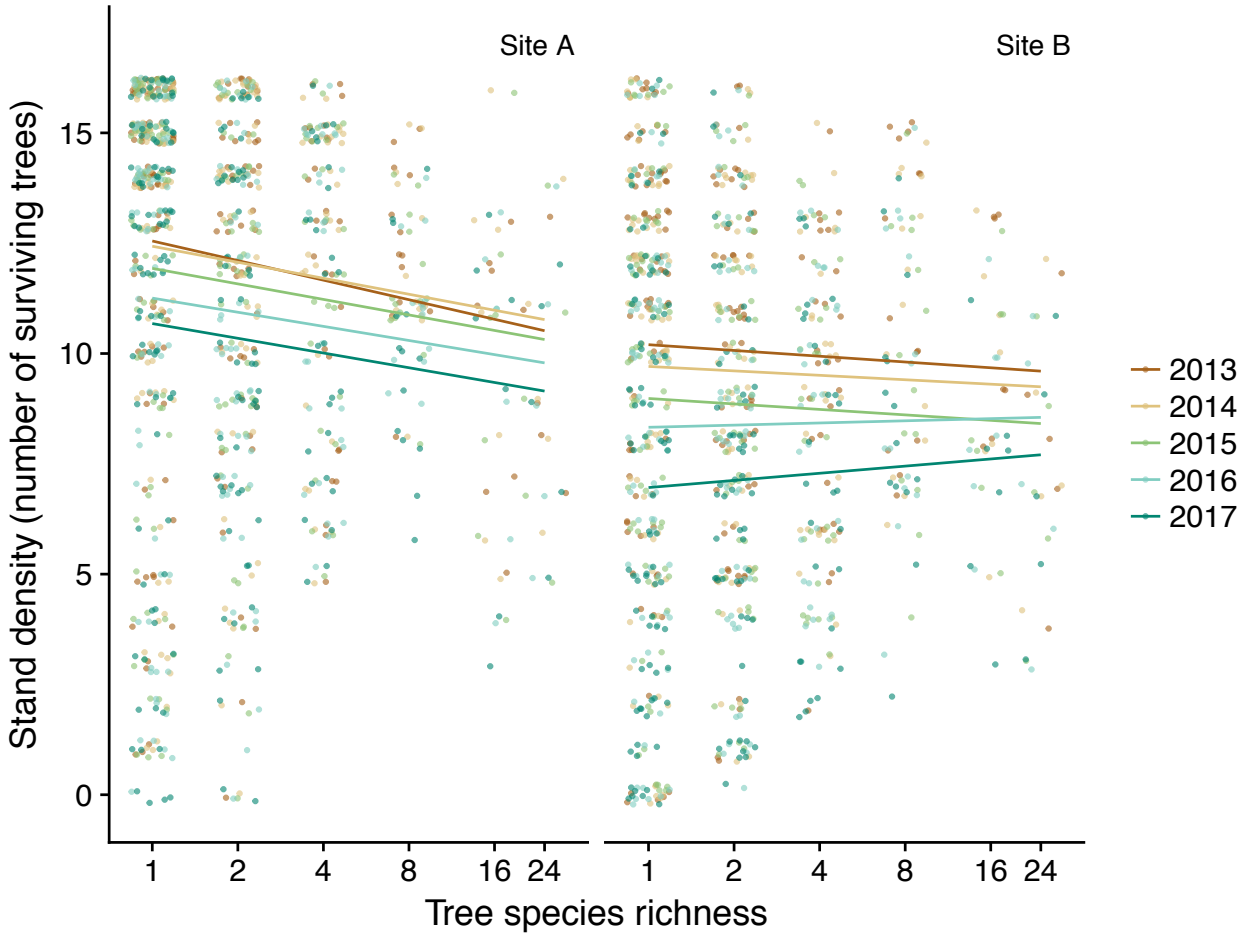

Fig. S6. Stand density as a function of tree species richness from 2013–2017. Raw data points are shown together with regression lines (for guidance only, effects of species richness and year by species richness interactions were not significant in mixed-model analysis: $P > 0.2$). Density indicates the number of surviving trees out of 16 planted in the central area of each plot.

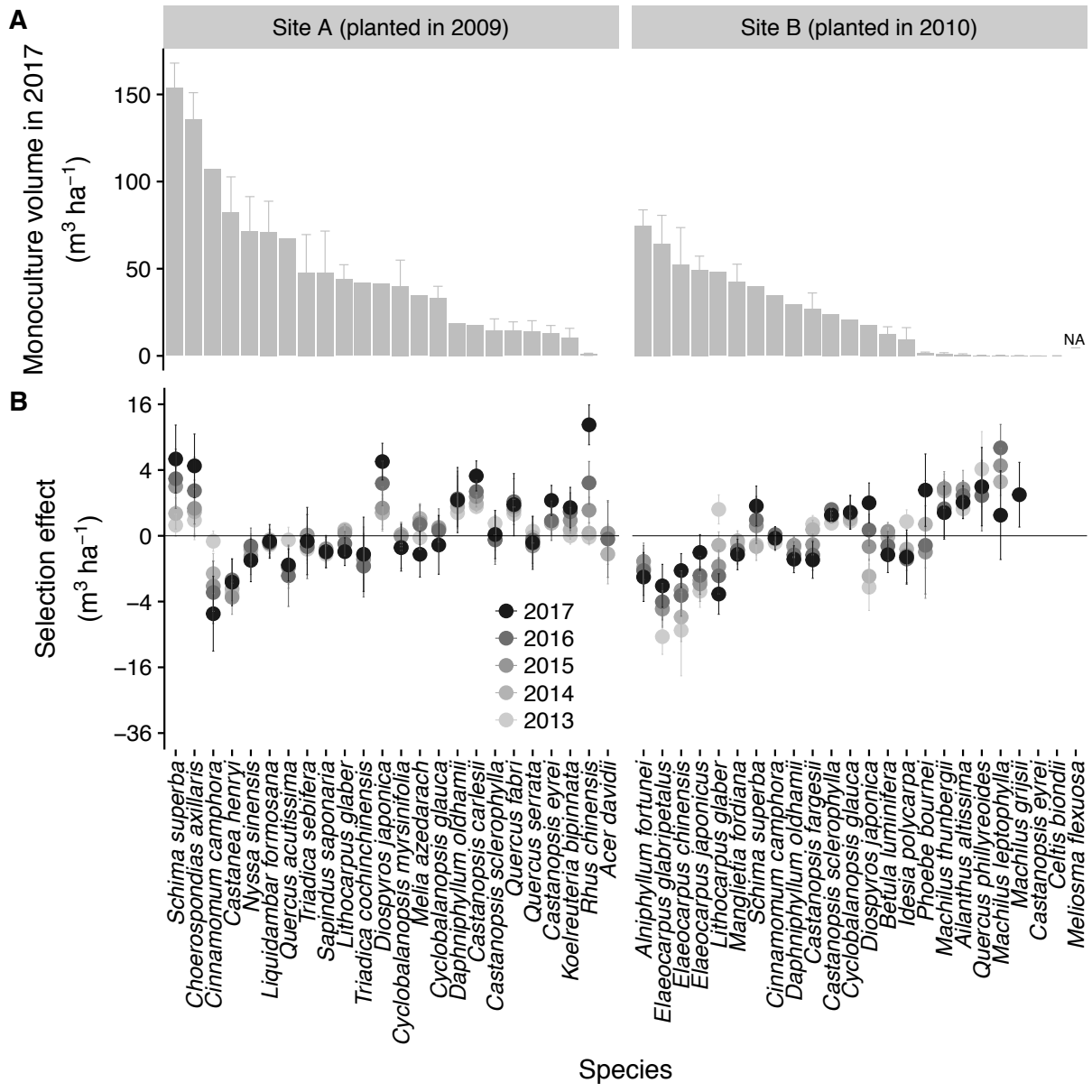

Fig. S7. Monoculture stand-level tree volume of species in 2017 (A) and species-specific selection effects (SEs) from 2013–2017 on stand-level tree volume (B). Plotted are means ± standard errors. The y-axis in B is square-root scaled to reflect the quadratic nature of selection effects *(10)*.

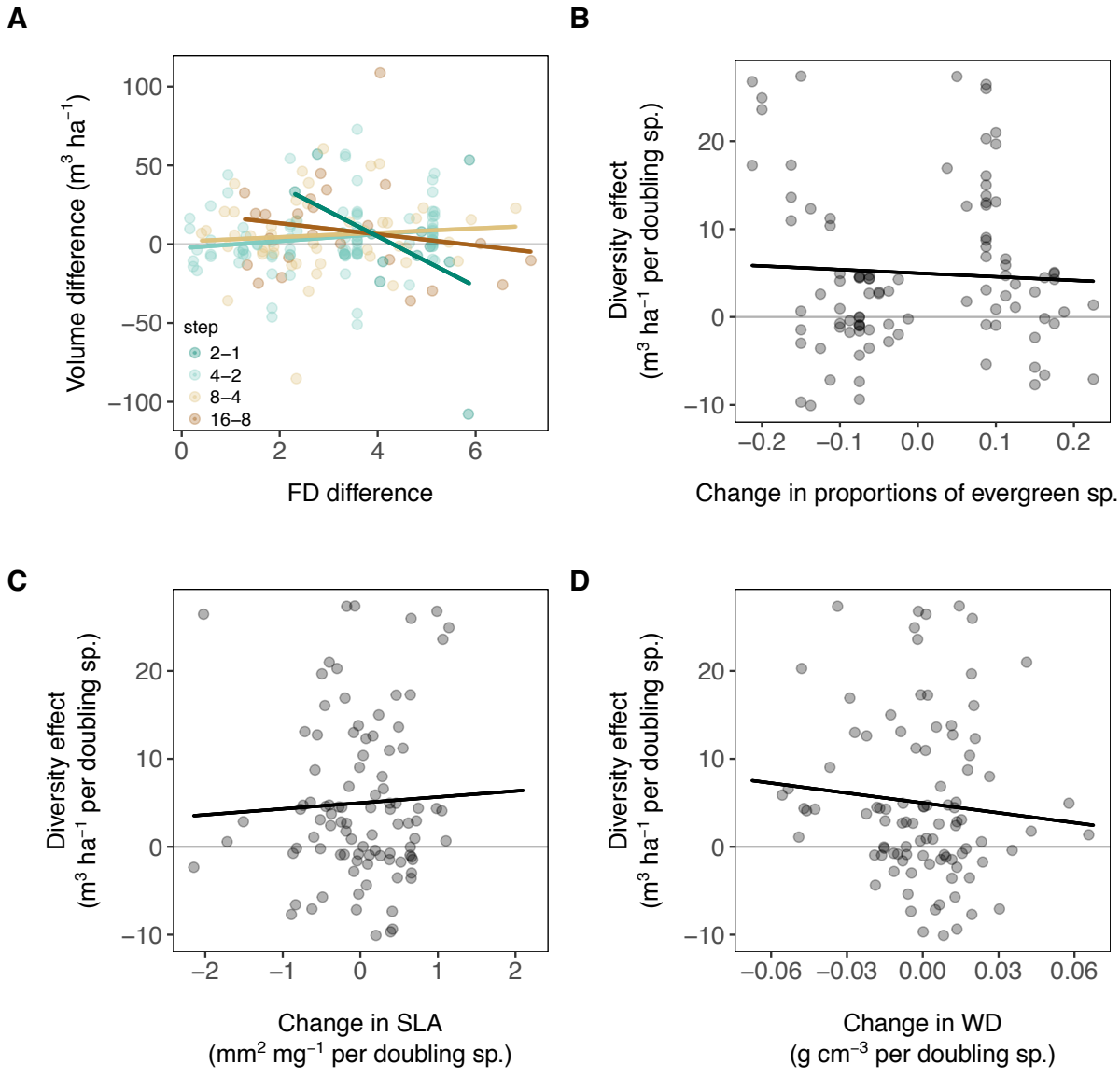

Fig. S8. Relationship between functional-trait trajectories of extinction sequences and reduction in stand volume when communities lose half of their species. In A, changes in functional trait diversity (FD) and volumes are shown separately for each step along the extinction sequences whereas in B–D slopes of stand volumes vs. $\log_2$-transformed species richness are shown for each extinction sequence with the given changes in community-weighted mean traits (Fig. S2). In A, slopes fitted for the different extinction steps decrease linearly from positive at low to negative at high richness ($F_{1,2} = 120.233$, $P = 0.008$), that is, high FD tends to increase volume gains at low species richness but to decrease them at high species richness. The slopes of the regression lines in B–D are not significantly different from zero ($P > 0.2$). Each point represents an average value across five years.

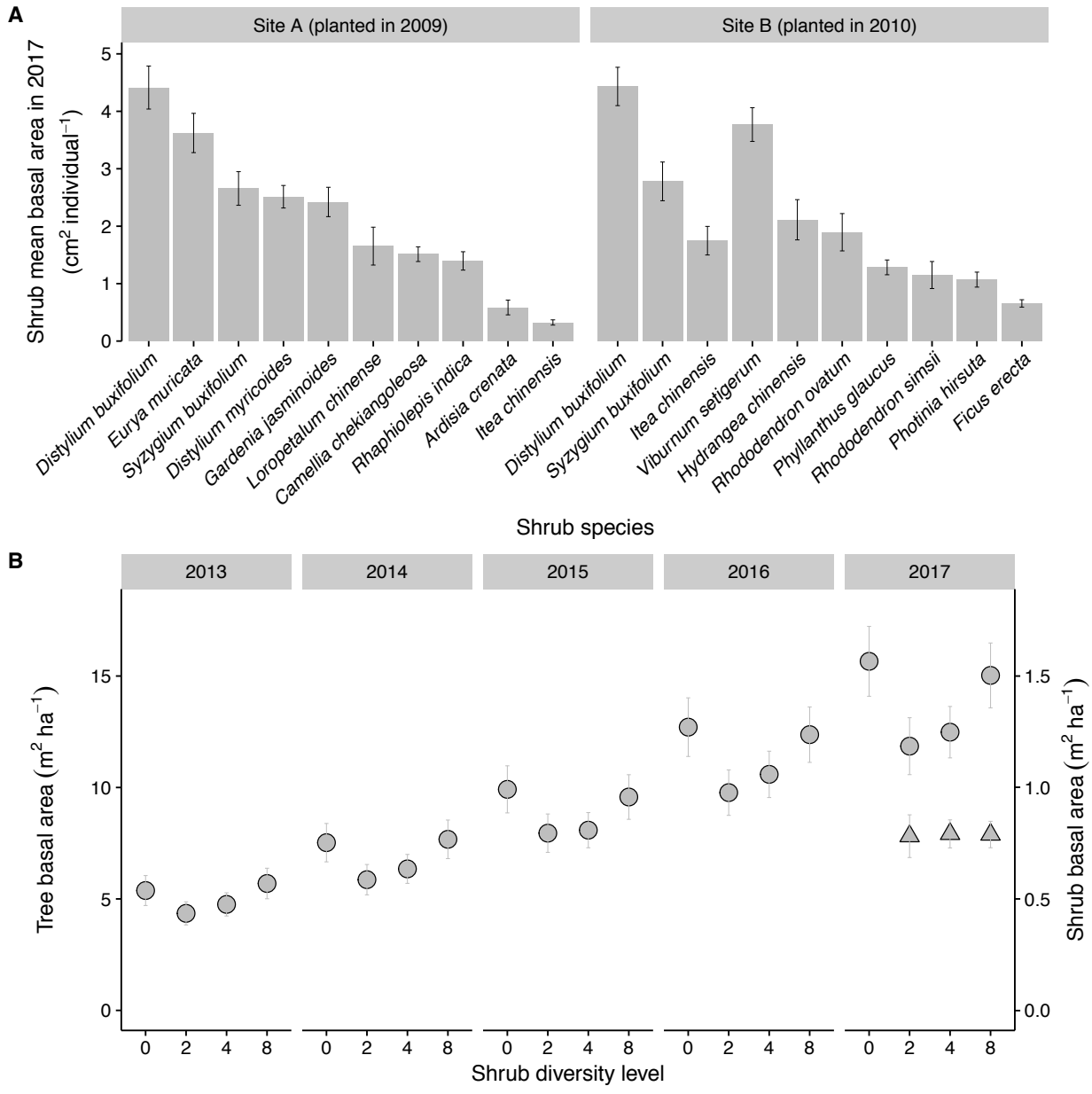

Fig. S9. Mean basal area of the longest ramet of the 18 shrub species used to assemble shrub-diversity treatments (A) and effects of shrub species richness on average stand-level tree basal area and shrub basal area (B). In B, stand-level basal areas of trees (circles, left y-axis) and understory shrubs (triangles, right y-axis; only data for 2017) are shown with means ± standard errors. Data are from species pools A1 and B1 (see Tables S1 and S2).

Table S1. Characteristics of tree species used in the BEF-China experiment. Information about sites and species pools refers to the design presented in Fig. S1 and Table S2. Information about other species characters was extracted from references *(36, 52-57)*. Initial height in m (means ± standard errors) was directly measured in the year of planting.

Species	Abbre-viation	Site	Pool	Leaf dur.	Shade	Succ. state	Habitat by description from floras	Initial height
Acer davidii Franchet	AcDa	A	A2, A3	D	I	I	streams, roadsides and sparse forest	25.8 ±3.7
Ailanthus altissima (Miller) Swingle	AiAl	B	B1, B3	D	I	E/I		62.4 ±5.0
Alniphyllum fortunei (Hemsley) Makino	AlFo	B	B1, B3	D	I	E	southern slopes of weed forest	32 ±1.2
Betula luminifera H. Winkler in Engler	BeLu	B	B1, B2	D	I	E	valleys, streams, piedmont and sunny mountain slopes	29.5 ±1.4
Castanea henryi (Skan) Rehd. et Wils.	CaHe	A	A1, A3	D	T	E		70.4 ±3.3
Castanopsis carlesii (Hemsley) Hayata	CaCa	A	A2, A3	E	T	L	mixed and evergreen broadleaf forest	12.5 ±4.4
Castanopsis eyrei (Champion ex Bentham) Tutcher	CaEy	AB	A1, A2, B1, B2	E	T	L	evergreen broadleaf forest or mixed coniferous and broadleaf forest, hills, dense or sparse montane forest	13.8 ±0.8
Castanopsis fargesii Franchet	CaFa	B	B1, B2	E	T	I/L	slopes and valleys	14.4 ±0.6
Castanopsis sclerophylla (Lindley & Paxton) Schottky	CaSc	AB	A1, A3, B2, B3	E	T	E/I/L		16.4 ±0.8
Celtis biondii Pampanini	CeBi	B	B1, B2	D	T	E/I		26.1 ±1.7
Choerospondias axillaris (Roxb.) Burtt et Hill	ChAx	A	A1, A3	D	I	E	lowland, hills and mountain forest	107.6 ±3.1
Cinnamomum camphora (Linnaeus) J. Presl in Berchtold & J. Presl	CiCa	AB	A2, A3, B2, B3	E	T	E/I/L		25.9 ±1.5
Cunninghamia lanceolata (Lamb.) Hook.	CuLa	AB		E	I	E		25.6 ±0.9
Cyclobalanopsis glauca (Thunberg) Oersted	CyGl	AB	A1, A3, B2, B3	E	T	I/L	slopes, streams and valleys, evergreen broadleaf forest or mixed mesophytic forest	12.3 ±0.7
Cyclobalanopsis myrsinifolia (Blume) Oersted	CyMy	A	A1, A2	E	T	I/L	lower montane broadleaf forest, mixed mesophytic forest in valleys	11.6 ±0.6
Daphniphyllum oldhamii (Hemsley) K. Rosenthal in Engler	DaOl	AB	A2, A3, B2, B3	E	T	L	slopes of broadleaf forest	19.4 ±1.1
Diospyros japonica Siebold & Zuccarini	DiJa	AB	A2, A3, B2, B3	D	I	E	valleys, slopes, mixed forest by streams in ravines	38.2 ±2.2
Elaeocarpus chinensis (Gardner & Champion) J. D. Hooker ex Bentham	ElCh	B	B1, B3	E	T	I/L	weed forest of mountain slopes, evergreen forest	26 ±1.3
Elaeocarpus glabripetalus Merrill	ElGl	B	B1, B3	E	T	I/L		31.9 ±1.3
Elaeocarpus japonicus Siebold & Zuccarini	ElJa	B	B1, B2	E	T	I/L	valleys, mountain slopes, streamsides, evergreen broadleaf forest	26.6 ±1.0

Idesia polycarpa Maximowicz	IdPo	B	B1, B3	D	I	E	sunny slopes, streamsides in the forest, deciduous broadleaf forest, mixed coniferous and broadleaf forest	29.3 ±1.4
Koelreuteria bipinnata Franch.	KoBi	A	A1, A2	D	I	E	slopes and streamsides, sparse forest	31.5 ±1.2
Liquidambar formosana Hance	LiFo	A	A1, A3	D	I	I		43 ±1.5
Lithocarpus glaber (Thunb.) Nakai	LiGl	AB	A1, A2, B1, B2	E	T	I/L	weed forest, mixed mesophytic forest, frequent on sunny slopes	18.1 ±0.6
Machilus grijsii Hance	MaGr	B	B1, B2	E	T	E/I	montane shrubland, dense forest or margins of forest, thickets	11.7 ±1.8
Machilus leptophylla Handel-Mazzetti	MaLe	B	B1, B2	E	T	I/L		11.1 ±0.5
Machilus thunbergii Siebold & Zuccarini	MaTh	B	B1, B3	E	T	I/L	mountain slopes or valleys, evergreen broadleaf forest	9 ±0.9
Manglietia fordiana Oliver	MaFo	B	B1, B2	E	T	I/L	hills, forest between rivers	18.6 ±0.7
Melia azedarach Linnaeus	MeAz	A	A2, A3	D	I	I		64 ±3.4
Meliosma flexuosa Pampanini	MeFl	B	B1, B3	D	I	E/I	submontane broadleaf forest or mixed coniferous and broadleaf forest	23.4 ±3.4
Nyssa sinensis Oliver	NySi	A	A1, A2	D	I	E	valleys, sunny slopes of wet broadleaf forest; wet mixed forest along valleys and streams	55.5 ±2.9
Phoebe bournei (Hemsley) Yen C. Yang	PhBo	B	B1, B3	E	T	I/L	mountain valleys, evergreen broadleaf forest	12.9 ±0.6
Pinus massoniana Lamb.	PiMa	AB		E	I	E/I		22.2 ±1.1
Quercus acutissima Carruthers	QuAc	A	A2, A3	D	I	E		42.4 ±4.6
Quercus fabri Hance	QuFa	A	A1, A2	D	I	E		25.6 ±1.5
Quercus phillyreoides A. Gray	QuPh	B	B1, B2	E	T	I/L	hills, submontane, bare rocks and cliffs, mixed mesophytic forest	17.6 ±3.3
Quercus serrata Murray	QuSe	A	A1, A3	D	I	E		37.7 ±1.6
Rhus chinensis Mill.	RhCh	A	A1, A3	D	I	E		47.7 ±2.2
Sapindus saponaria Linnaeus	SaSa	A	A1, A2	D	I	E	slopes, streamsides and ravines, margins of forest	52.5 ±1.9
Schima superba Gardn. et Champ.	ScSu	AB	A1, A2, B1, B2	E	T	E/I/L		33.1 ±1.1
Triadica cochinchinensis Loureiro	TrCo	A	A2, A3	D	I	E	moist evergreen broadleaf forest, montane forest or brushwood	85.1 ±13.7
Triadica sebifera (L.) Small	TrSe	A	A1, A3	D	I	E	forest on limestone	71.4 ±2.3

Notes: leaf dur(ation) D = deciduous, E = evergreen; shade (tolerance) I = intolerant, T = tolerant, succ(essional) stage E = early, I = intermediate, L = late.

Table S2. Experimental design.

Site	Pool	Species richness	Plot size	Shrub treatment	Species composition
A	A1	16	4mu/1mu	yes	CyGl QuFa RhCh ScSu CaEy CyMy KoBi LiGl CaHe NySi LiFo SaSa CaSc QuSe ChAx TrSe
		8	4mu/1mu	yes	CyGl QuFa RhCh ScSu CaEy CyMy KoBi LiGl CaHe NySi LiFo SaSa CaSc QuSe ChAx TrSe
		4	4mu/1mu	yes	CyGl QuFa RhCh ScSu CaEy CyMy KoBi LiGl CaHe NySi LiFo SaSa CaSc QuSe ChAx TrSe
		2	4mu/1mu	yes	CyGl QuFa RhCh ScSu CaEy CyMy KoBi LiGl CaHe NySi LiFo SaSa CaSc QuSe ChAx TrSe
		1	4mu/1mu	yes	CyGl QuFa RhCh ScSu CaEy CyMy KoBi LiGl CaHe NySi LiFo SaSa CaSc QuSe ChAx TrSe
	A2	16	1mu	no	CaCa LiGl AcDa MeAz CaEy KoBi CiCa CyMy DiJa NySi TrCo ScSu DaOl QuFa QuAc SaSa
		8	1mu	no	CaCa LiGl AcDa MeAz CaEy KoBi CiCa CyMy DiJa NySi TrCo ScSu DaOl QuFa QuAc SaSa
		4	1mu	no	CaCa LiGl AcDa MeAz CaEy KoBi CiCa CyMy DiJa NySi TrCo ScSu DaOl QuFa QuAc SaSa
		2	1mu	no	CaCa LiGl AcDa MeAz CaEy KoBi CiCa CyMy DiJa NySi TrCo ScSu DaOl QuFa QuAc SaSa
		1	1mu	no	CaCa LiGl AcDa MeAz CaEy KoBi CiCa CyMy DiJa NySi TrCo ScSu DaOl QuFa QuAc SaSa
	A3	16	1mu	no	AcDa QuAc CaHe RhCh CaSc CiCa LiFo MeAz CaCa CyGl TrCo TrSe ChAx DiJa DaOl QuSe
		8	1mu	no	AcDa QuAc CaHe RhCh CaSc CiCa LiFo MeAz CaCa CyGl TrCo TrSe ChAx DiJa DaOl QuSe
		4	1mu	no	AcDa QuAc CaHe RhCh CaSc CiCa LiFo MeAz CaCa CyGl TrCo TrSe ChAx DiJa DaOl QuSe
		2	1mu	no	AcDa QuAc CaHe RhCh CaSc CiCa LiFo MeAz CaCa CyGl TrCo TrSe ChAx DiJa DaOl QuSe
		1	1mu	no	AcDa QuAc CaHe RhCh CaSc CiCa LiFo MeAz CaCa CyGl TrCo TrSe ChAx DiJa DaOl QuSe
B	B1	16	4mu/1mu	yes	AiAl MeFl IdPo MaGr CeBi ElGl ElJa PhBo BeLu CaFa MaFo QuPh ElCh MaTh AlFo MaLe
		8	4mu/1mu	yes	AiAl MeFl IdPo MaGr CeBi ElGl ElJa PhBo BeLu CaFa MaFo QuPh ElCh MaTh AlFo MaLe
		4	4mu/1mu	yes	AiAl MeFl IdPo MaGr CeBi ElGl ElJa PhBo BeLu CaFa MaFo QuPh ElCh MaTh AlFo MaLe
		2	4mu/1mu	yes	AiAl MeFl IdPo MaGr CeBi ElGl ElJa PhBo BeLu CaFa MaFo QuPh ElCh MaTh AlFo MaLe
		1	4mu/1mu	yes	AiAl MeFl IdPo MaGr CeBi ElGl ElJa PhBo BeLu CaFa MaFo QuPh ElCh MaTh AlFo MaLe
	B2	16	1mu	no	CaEy CeBi MaLe PhBo DiJa LiGl ElGl MaTh AiAl AlFo CaFa CaSc CyGl ScSu CiCa DaOl
		8	1mu	no	CaEy CeBi MaLe PhBo DiJa LiGl ElGl MaTh AiAl AlFo CaFa CaSc CyGl ScSu CiCa DaOl
		4	1mu	no	CaEy CeBi MaLe PhBo DiJa LiGl ElGl MaTh AiAl AlFo CaFa CaSc CyGl ScSu CiCa DaOl
		2	1mu	no	CaEy CeBi MaLe PhBo DiJa LiGl ElGl MaTh AiAl AlFo CaFa CaSc CyGl ScSu CiCa DaOl
		1	1mu	no	CaEy CeBi MaLe PhBo DiJa LiGl ElGl MaTh AiAl AlFo CaFa CaSc CyGl ScSu CiCa DaOl
	B3	16	1mu	no	BeLu DaOl CaEy QuPh CyGl MaGr ElJa LiGl CaSc IdPo ElCh MaFo CiCa DiJa MeFl ScSu
		8	1mu	no	BeLu DaOl CaEy QuPh CyGl MaGr ElJa LiGl CaSc IdPo ElCh MaFo CiCa DiJa MeFl ScSu
		4	1mu	no	BeLu DaOl CaEy QuPh CyGl MaGr ElJa LiGl CaSc IdPo ElCh MaFo CiCa DiJa MeFl ScSu
		2	1mu	no	BeLu DaOl CaEy QuPh CyGl MaGr ElJa LiGl CaSc IdPo ElCh MaFo CiCa DiJa MeFl ScSu
		1	1mu	no	BeLu DaOl CaEy QuPh CyGl MaGr ElJa LiGl CaSc IdPo ElCh MaFo CiCa DiJa MeFl ScSu

Note: See Table S1 for species abbreviations.

Table S3. Summary statistics from mixed-effects models assessing the effects of functional-trait diversity measures (*44, 45*) and species richness (logSR) on stand volume from 2013–2017. Left side measures based on seven functional traits, right side measures based on three functional traits.

Seven traits	df	ddf	F	*P*	Three traits	df	ddf	F	*P*
Model 1									
Site	1	99.7	20.68	<0.001	Site	1	99.9	20.71	<0.001
FD	1	81.6	6.59	0.012	FD	1	81.6	6.33	0.014
LogSR	1	107.3	0.10	0.755	LogSR	1	113.6	0.36	0.550
Year	4	393.8	196.9	<0.001	Year	4	396.6	196.6	<0.001
Site × year	4	407.2	20.80	<0.001	Site ×year	4	408.9	20.84	<0.001
FD × year	4	335.1	12.48	<0.001	FD ×year	4	335.9	11.73	<0.001
LogSR ×year	4	441.4	0.08	0.988	LogSR ×year	4	470.0	0.58	0.678
Model 2									
Site	1	99.7	20.68	<0.001	Site	1	99.7	20.71	<0.001
LogSR	1	87.5	6.58	0.012	LogSR	1	87.8	6.59	0.012
FD	1	99.8	0.11	0.746	FD	1	104.6	0.09	0.760
Year	4	393.8	196.9	<0.001	Year	4	396.6	196.6	<0.001
Site ×year	4	407.2	20.80	<0.001	Site ×year	4	408.9	20.84	<0.001
LogSR ×year	4	360.8	11.95	<0.001	LogSR ×year	4	363.5	11.94	<0.001
FD ×year	4	410.3	0.61	0.654	FD ×year	4	429.7	0.37	0.829
Model 1									
Site	1	99.9	20.71	<0.001	Site	1	99.7	20.68	<0.001
FDis	1	85.9	3.77	0.055	FDis	1	80.8	4.66	0.034
LogSR	1	93.7	2.82	0.096	LogSR	1	88.8	2.05	0.156
Year	4	398.7	195.7	<0.001	Year	4	396.6	196.2	<0.001
Site × year	4	409.9	20.82	<0.001	Site ×year	4	408.9	20.83	<0.001
FDis × year	4	357.3	6.80	<0.001	FDis ×year	4	335.1	8.52	<0.001
LogSR ×year	4	389.9	5.14	<0.001	LogSR ×year	4	368.1	3.68	0.006
Model 2									
Site	1	99.9	20.71	<0.001	Site	1	99.7	20.68	<0.001
LogSR	1	88.0	6.58	0.012	LogSR	1	87.5	6.58	0.012
FDis	1	91.5	0.010	0.919	FDis	1	81.8	0.12	0.729
Year	4	398.7	195.7	<0.001	Year	4	396.6	196.2	<0.001
Site ×year	4	409.9	20.82	<0.001	Site ×year	4	408.9	20.83	<0.001
LogSR ×year	4	365.7	11.89	<0.001	LogSR ×year	4	363.7	11.92	<0.001
FDis ×year	4	380.9	0.041	0.997	FDis ×year	4	338.1	0.27	0.894

Note: FD is Petchey and Gaston's functional diversity (*44*); FDis is functional dispersion (*45*). Abbreviations: df = numerator degrees of freedom; ddf = denominator degrees of freedom. F and *P* indicate F-ratios and *P*-values of the significance tests.

Table S4. Summary statistics from mixed-effects models assessing the effects of phylogenetic diversity measures (*48*) and species richness (logSR) on stand volume from 2013–2017.

	df	ddf	F	*P*
Model 1				
Site	1	99.7	20.67	<0.001
PD	1	78.6	5.79	0.018
LogSR	1	97.9	0.79	0.375
Year	4	395.3	196.0	<0.001
Site × year	4	408.3	20.80	<0.001
PD × year	4	324.8	10.20	<0.001
LogSR ×year	4	405.6	1.85	0.118
Model 2				
Site	1	99.7	20.67	<0.001
LogSR	1	87.4	6.57	0.012
PD	1	88.1	0.02	0.902
Year	4	395.3	196.0	<0.001
Site ×year	4	408.3	20.80	<0.001
LogSR ×year	4	362.4	11.90	<0.001
PD ×year	4	364.7	0.16	0.959
Model 1				
Site	1	99.4	20.93	<0.001
MPD	1	84.2	8.61	0.004
LogSR	1	93.8	0.55	0.459
Year	4	400.2	198.1	<0.001
Site × year	4	408.6	21.06	<0.001
MPD × year	4	348.7	11.71	<0.001
LogSR ×year	4	390.7	2.31	0.057
Model 2				
Site	1	99.4	20.93	<0.001
LogSR	1	88.2	6.66	0.011
MPD	1	89.4	2.50	0.117
Year	4	400.2	198.1	<0.001
Site ×year	4	408.6	21.06	<0.001
LogSR ×year	4	367.0	12.05	<0.001
MPD ×year	4	370.8	1.97	0.098

Notes: PD is Faith's phylogenetic diversity; MPD is mean pairwise phylogenetic distance. Abbreviations: df = numerator degrees of freedom; ddf = denominator degrees of freedom. F and *P* indicate F-ratios and *P*-values of the significance tests.

Table S5. Summary statistics from mixed-effects models assessing the temporal change of the relationships between trait distance (TD) and biodiversity effects on stand volume in two-species mixtures. TDs were calculated with leaf duration, specific leaf area (SLA) and wood density (WD), and jointly with the three z-transformed traits (multivariate TD). Biodiversity effects obtained by additive partitioning were analyzed: net biodiversity effect (NE), complementarity effect (CE) and selection effect (SE).

	NE				CE				SE			
	df	ddf	F	*P*	df	ddf	F	*P*	df	ddf	F	*P*
Leaf duration												
TD	1	26.3	0.070	0.793	1	23.6	0.492	0.490	1	25.9	2.717	0.111
Year	4	74.4	1.054	0.385	4	100.2	0.587	0.673	4	107.2	0.393	0.813
TD × year	4	68.9	1.757	0.148	4	93.0	3.921	0.006	4	99.4	3.378	0.012
SLA												
TD	1	34.8	0.841	0.366	1	32.2	2.411	0.130	1	35.0	0.922	0.344
Year	4	82.9	0.924	0.454	4	86.8	0.718	0.582	4	102.5	0.433	0.785
TD × year	4	83.8	0.824	0.514	4	88.5	6.745	<0.001	4	103.4	2.275	0.066
WD												
TD	1	33.7	0.943	0.338	1	38.0	0.706	0.406	1	33.2	0.010	0.919
Year	4	74.4	0.970	0.429	4	104.6	0.580	0.678	4	110.6	0.363	0.835
TD × year	4	102.0	1.673	0.162	4	136.5	1.359	0.251	4	138.6	0.406	0.804
Multivariate TD												
TD	1	36.4	1.540	0.223	1	36.3	2.609	0.115	1	33.4	1.119	0.298
Year	4	76.4	1.069	0.378	4	84.8	0.844	0.501	4	102.5	0.432	0.785
TD × year	4	101.2	3.325	0.013	4	118.1	9.300	<0.001	4	123.4	3.571	0.009

Notes: biodiversity effects were square-root transformed with sign reconstruction ($\text{sign}(y)\sqrt{|y|}$). TD, year and their interaction were fitted after site [for random terms see (*24*)]. Abbreviations: df = numerator degrees of freedom; ddf = denominator degrees of freedom. F and *P* indicate F-ratios and *P*-values of the significance tests.

References and Notes

1. A. S. Mori, Environmental controls on the causes and functional consequences of tree species diversity. *J. Ecol.* **106**, 113–125 (2018). doi:10.1111/1365-2745.12851

2. L. Gamfeldt, T. Snäll, R. Bagchi, M. Jonsson, L. Gustafsson, P. Kjellander, M. C. Ruiz-Jaen, M. Fröberg, J. Stendahl, C. D. Philipson, G. Mikusiński, E. Andersson, B. Westerlund, H. Andrén, F. Moberg, J. Moen, J. Bengtsson, Higher levels of multiple ecosystem services are found in forests with more tree species. *Nat. Commun.* **4**, 1340 (2013). doi:10.1038/ncomms2328 Medline

3. J. Liang, T. W. Crowther, N. Picard, S. Wiser, M. Zhou, G. Alberti, E.-D. Schulze, A. D. McGuire, F. Bozzato, H. Pretzsch, S. de-Miguel, A. Paquette, B. Hérault, M. Scherer-Lorenzen, C. B. Barrett, H. B. Glick, G. M. Hengeveld, G.-J. Nabuurs, S. Pfautsch, H. Viana, A. C. Vibrans, C. Ammer, P. Schall, D. Verbyla, N. Tchebakova, M. Fischer, J. V. Watson, H. Y. H. Chen, X. Lei, M.-J. Schelhaas, H. Lu, D. Gianelle, E. I. Parfenova, C. Salas, E. Lee, B. Lee, H. S. Kim, H. Bruelheide, D. A. Coomes, D. Piotto, T. Sunderland, B. Schmid, S. Gourlet-Fleury, B. Sonké, R. Tavani, J. Zhu, S. Brandl, J. Vayreda, F. Kitahara, E. B. Searle, V. J. Neldner, M. R. Ngugi, C. Baraloto, L. Frizzera, R. Bałazy, J. Oleksyn, T. Zawiła-Niedźwiecki, O. Bouriaud, F. Bussotti, L. Finér, B. Jaroszewicz, T. Jucker, F. Valladares, A. M. Jagodzinski, P. L. Peri, C. Gonmadje, W. Marthy, T. O'Brien, E. H. Martin, A. R. Marshall, F. Rovero, R. Bitariho, P. A. Niklaus, P. Alvarez-Loayza, N. Chamuya, R. Valencia, F. Mortier, V. Wortel, N. L. Engone-Obiang, L. V. Ferreira, D. E. Odeke, R. M. Vasquez, S. L. Lewis, P. B. Reich, Positive biodiversity-productivity relationship predominant in global forests. *Science* **354**, eaaf8957 (2016). doi:10.1126/science.aaf8957 Medline

4. A. Hector, B. Schmid, C. Beierkuhnlein, M. C. Caldeira, M. Diemer, P. G. Dimitrakopoulos, J. A. Finn, H. Freitas, P. S. Giller, J. Good, R. Harris, P. Hogberg, K. Huss-Danell, J. Joshi, A. Jumpponen, C. Korner, P. W. Leadley, M. Loreau, A. Minns, C. P. Mulder, G. O'Donovan, S. J. Otway, J. S. Pereira, A. Prinz, D. J. Read, l. et, Plant diversity and productivity experiments in european grasslands. *Science* **286**, 1123–1127 (1999). doi:10.1126/science.286.5442.1123 Medline

5. P. B. Reich, D. Tilman, F. Isbell, K. Mueller, S. E. Hobbie, D. F. B. Flynn, N. Eisenhauer, Impacts of biodiversity loss escalate through time as redundancy fades. *Science* **336**, 589–592 (2012). doi:10.1126/science.1217909 Medline

6. D. Tilman, D. Wedin, J. Knops, Productivity and sustainability influenced by biodiversity in grassland ecosystems. *Nature* **379**, 718–720 (1996). doi:10.1038/379718a0

7. D. Tilman, C. L. Lehman, K. T. Thomson, Plant diversity and ecosystem productivity: Theoretical considerations. *Proc. Natl. Acad. Sci. U.S.A.* **94**, 1857–1861 (1997). doi:10.1073/pnas.94.5.1857 Medline

8. S. A. Schnitzer, J. N. Klironomos, J. Hillerislambers, L. L. Kinkel, P. B. Reich, K. Xiao, M. C. Rillig, B. A. Sikes, R. M. Callaway, S. A. Mangan, E. H. van Nes, M. Scheffer, Soil microbes drive the classic plant diversity-productivity pattern. *Ecology* **92**, 296–303 (2011). doi:10.1890/10-0773.1 Medline

9. M. A. Huston, Hidden treatments in ecological experiments: Re-evaluating the ecosystem function of biodiversity. *Oecologia* **110**, 449–460 (1997). doi:10.1007/s004420050180 Medline

10. M. Loreau, A. Hector, Partitioning selection and complementarity in biodiversity experiments. *Nature* **412**, 72–76 (2001). doi:10.1038/35083573 Medline

11. H. Bruelheide, M. Böhnke, S. Both, T. Fang, T. Assmann, M. Baruffol, J. Bauhus, F. Buscot, X.-Y. Chen, B.-Y. Ding, W. Durka, A. Erfmeier, M. Fischer, C. Geißler, D. Guo, L.-D. Guo, W. Härdtle, J.-S. He, A. Hector, W. Kröber, P. Kühn, A. C. Lang, K. Nadrowski, K. Pei, M. Scherer-Lorenzen, X. Shi, T. Scholten, A. Schuldt, S. Trogisch, G. von Oheimb, E. Welk, C. Wirth, Y.-T. Wu, X. Yang, X. Zeng, S. Zhang, H. Zhou, K. Ma, B. Schmid, Community assembly during secondary forest succession in a Chinese subtropical forest. *Ecol. Monogr.* **81**, 25–41 (2011). doi:10.1890/09-2172.1

12. S. P. Hubbell, Neutral theory and the evolution of ecological equivalence. *Ecology* **87**, 1387–1398 (2006). doi:10.1890/0012-9658(2006)87[1387:NTATEO]2.0.CO;2 Medline

13. X. Wang, T. Wiegand, N. J. B. Kraft, N. G. Swenson, S. J. Davies, Z. Hao, R. Howe, Y. Lin, K. Ma, X. Mi, S.-H. Su, I.-F. Sun, A. Wolf, Stochastic dilution effects weaken deterministic effects of niche-based processes in species rich forests. *Ecology* **97**, 347–360 (2016). doi:10.1890/14-2357.1 Medline

14. M. Scherer-Lorenzen, "The functional role of biodiversity in the context of global change" in *Forests and Global Change*, D. A. Coomes, D. F. R. P. Burslem, W. D. Simonson, Eds. (Cambridge Univ. Press, 2014), pp. 195–238.

15. K. Verheyen, M. Vanhellemont, H. Auge, L. Baeten, C. Baraloto, N. Barsoum, S. Bilodeau-Gauthier, H. Bruelheide, B. Castagneyrol, D. Godbold, J. Haase, A. Hector, H. Jactel, J. Koricheva, M. Loreau, S. Mereu, C. Messier, B. Muys, P. Nolet, A. Paquette, J. Parker, M. Perring, Q. Ponette, C. Potvin, P. Reich, A. Smith, M. Weih, M. Scherer-Lorenzen, Contributions of a global network of tree diversity experiments to sustainable forest plantations. *Ambio* **45**, 29–41 (2016). doi:10.1007/s13280-015-0685-1 Medline

16. J. J. Grossman, J. Cavender-Bares, S. E. Hobbie, P. B. Reich, R. A. Montgomery, Species richness and traits predict overyielding in stem growth in an early-successional tree diversity experiment. *Ecology* **98**, 2601–2614 (2017). doi:10.1002/ecy.1958 Medline

17. C. Potvin, N. J. Gotelli, Biodiversity enhances individual performance but does not affect survivorship in tropical trees. *Ecol. Lett.* **11**, 217–223 (2008). doi:10.1111/j.1461-0248.2007.01148.x Medline

18. J. Sapijanskas, A. Paquette, C. Potvin, N. Kunert, M. Loreau, Tropical tree diversity enhances light capture through crown plasticity and spatial and temporal niche differences. *Ecology* **95**, 2479–2492 (2014). doi:10.1890/13-1366.1

19. C. M. Tobner, A. Paquette, D. Gravel, P. B. Reich, L. J. Williams, C. Messier, Functional identity is the main driver of diversity effects in young tree communities. *Ecol. Lett.* **19**, 638–647 (2016). doi:10.1111/ele.12600 Medline

20. T. Van de Peer, K. Verheyen, Q. Ponette, N. N. Setiawan, B. Muys, Overyielding in young tree plantations is driven by local complementarity and selection effects related to shade tolerance. *J. Ecol.* **106**, 1096–1105 (2017). doi:10.1111/1365-2745.12839

21. L. J. Williams, A. Paquette, J. Cavender-Bares, C. Messier, P. B. Reich, Spatial complementarity in tree crowns explains overyielding in species mixtures. *Nat. Ecol. Evol.* **1**, 63 (2017). doi:10.1038/s41559-016-0063 Medline

22. D. A. Clarke, P. H. York, M. A. Rasheed, T. D. Northfield, Does biodiversity–ecosystem function literature neglect tropical ecosystems? *Trends Ecol. Evol.* **32**, 320–323 (2017). doi:10.1016/j.tree.2017.02.012 Medline

23. H. Bruelheide, K. Nadrowski, T. Assmann, J. Bauhus, S. Both, F. Buscot, X.-Y. Chen, B. Ding, W. Durka, A. Erfmeier, J. L. M. Gutknecht, D. Guo, L.-D. Guo, W. Härdtle, J.-S. He, A.-M. Klein, P. Kühn, Y. Liang, X. Liu, S. Michalski, P. A. Niklaus, K. Pei, M. Scherer-Lorenzen, T. Scholten, A. Schuldt, G. Seidler, S. Trogisch, G. von Oheimb, E. Welk, C. Wirth, T. Wubet, X. Yang, M. Yu, S. Zhang, H. Zhou, M. Fischer, K. Ma, B. Schmid, Designing forest biodiversity experiments: General considerations illustrated by a new large experiment in subtropical China. *Methods Ecol. Evol.* **5**, 74–89 (2014). doi:10.1111/2041-210X.12126

24. Materials and methods are available as supplementary materials.

25. P. B. Adler, A. Fajardo, A. R. Kleinhesselink, N. J. B. Kraft, Trait-based tests of coexistence mechanisms. *Ecol. Lett.* **16**, 1294–1306 (2013). doi:10.1111/ele.12157 Medline

26. S. Greenwood, P. Ruiz-Benito, J. Martínez-Vilalta, F. Lloret, T. Kitzberger, C. D. Allen, R. Fensham, D. C. Laughlin, J. Kattge, G. Bönisch, N. J. B. Kraft, A. S. Jump, Tree mortality across biomes is promoted by drought intensity, lower wood density and higher specific leaf area. *Ecol. Lett.* **20**, 539–553 (2017). doi:10.1111/ele.12748 Medline

27. E. Marquard, A. Weigelt, C. Roscher, M. Gubsch, A. Lipowsky, B. Schmid, Positive biodiversity-productivity relationship due to increased plant density. *J. Ecol.* **97**, 696–704 (2009). doi:10.1111/j.1365-2745.2009.01521.x

28. D. F. B. Flynn, N. Mirotchnick, M. Jain, M. I. Palmer, S. Naeem, Functional and phylogenetic diversity as predictors of biodiversity–ecosystem-function relationships. *Ecology* **92**, 1573–1581 (2011). doi:10.1890/10-1245.1 Medline

29. T. Jucker, O. Bouriaud, D. A. Coomes, Crown plasticity enables trees to optimize canopy packing in mixed-species forests. *Funct. Ecol.* **29**, 1078–1086 (2015). doi:10.1111/1365-2435.12428

30. P. A. Niklaus, M. Baruffol, J.-S. He, K. Ma, B. Schmid, Can niche plasticity promote biodiversity-productivity relationships through increased complementarity? *Ecology* **98**, 1104–1116 (2017). doi:10.1002/ecy.1748 Medline

31. R. G. Wagner, K. M. Little, B. Richardson, K. McNabb, The role of vegetation management for enhancing productivity of the world's forests. *Forestry* **79**, 57–79 (2006). doi:10.1093/forestry/cpi057

32. F. Isbell, A. Gonzalez, M. Loreau, J. Cowles, S. Díaz, A. Hector, G. M. Mace, D. A. Wardle, M. I. O'Connor, J. E. Duffy, L. A. Turnbull, P. L. Thompson, A. Larigauderie, Linking the influence and dependence of people on biodiversity across scales. *Nature* **546**, 65–72 (2017). doi:10.1038/nature22899 Medline

33. Food and Agriculture Organization of the United Nations (FAO), *Global Forest Resources Assessment* (FAO, 2015).

34. R. J. Keenan, G. A. Reams, F. Achard, J. V. de Freitas, A. Grainger, E. Lindquist, Dynamics of global forest area: Results from the FAO Global Forest Resources Assessment 2015. *For. Ecol. Manage.* **352**, 9–20 (2015). doi:10.1016/j.foreco.2015.06.014

35. F. Hua, X. Wang, X. Zheng, B. Fisher, L. Wang, J. Zhu, Y. Tang, D. W. Yu, D. S. Wilcove, Opportunities for biodiversity gains under the world's largest reforestation programme. *Nat. Commun.* **7**, 12717 (2016). doi:10.1038/ncomms12717 Medline

36. X. Yang, J. Bauhus, S. Both, T. Fang, W. Härdtle, W. Kröber, K. Ma, K. Nadrowski, K. Pei, M. Scherer-Lorenzen, T. Scholten, G. Seidler, B. Schmid, G. von Oheimb, H. Bruelheide, Establishment success in a forest biodiversity and ecosystem functioning experiment in subtropical China (BEF-China). *Eur. J. For. Res.* **132**, 593–606 (2013). doi:10.1007/s10342-013-0696-z

37. Climate data from National Meteorological Information Center, China Meteorological Administration; http://data.cma.cn.

38. A. R. Martin, S. C. Thomas, A reassessment of carbon content in tropical trees. *PLOS ONE* **6**, e23533 (2011). doi:10.1371/journal.pone.0023533 Medline

39. M. Brezzi, thesis, University of Zurich, 2015.

40. M. Plummer, rjags-package: Bayesian graphical models using MCMC. R package version 4-6. (2016).

41. A. Gelman, D. B. Rubin, Inference from iterative simulation using multiple sequences. *Stat. Sci.* **7**, 457–472 (1992). doi:10.1214/ss/1177011136

42. E. Marquard, A. Weigelt, V. M. Temperton, C. Roscher, J. Schumacher, N. Buchmann, M. Fischer, W. W. Weisser, B. Schmid, Plant species richness and functional composition drive overyielding in a six-year grassland experiment. *Ecology* **90**, 3290–3302 (2009). doi:10.1890/09-0069.1 Medline

43. W. Kröber, Y. Li, W. Härdtle, K. Ma, B. Schmid, K. Schmidt, T. Scholten, G. Seidler, G. von Oheimb, E. Welk, C. Wirth, H. Bruelheide, Early subtropical forest growth is driven by community mean trait values and functional diversity rather than the abiotic environment. *Ecol. Evol.* **5**, 3541–3556 (2015). doi:10.1002/ece3.1604 Medline

44. O. L. Petchey, K. J. Gaston, Functional diversity (FD), species richness and community composition. *Ecol. Lett.* **5**, 402–411 (2002). doi:10.1046/j.1461-0248.2002.00339.x

45. E. Laliberté, P. Legendre, A distance-based framework for measuring functional diversity from multiple traits. *Ecology* **91**, 299–305 (2010). doi:10.1890/08-2244.1 Medline

46. B. F. Chabot, D. J. Hicks, The ecology of leaf life spans. *Annu. Rev. Ecol. Syst.* **13**, 229–259 (1982). doi:10.1146/annurev.es.13.110182.001305

47. S. J. Wright, K. Kitajima, N. J. B. Kraft, P. B. Reich, I. J. Wright, D. E. Bunker, R. Condit, J. W. Dalling, S. J. Davies, S. Díaz, B. M. J. Engelbrecht, K. E. Harms, S. P. Hubbell, C. O. Marks, M. C. Ruiz-Jaen, C. M. Salvador, A. E. Zanne, Functional traits and the growth-

mortality trade-off in tropical trees. *Ecology* **91**, 3664–3674 (2010). doi:10.1890/09-2335.1 Medline

48. M. Vellend, W. K. Cornwell, K. Magnuson-Ford, A. Ø. Mooers, Measuring phylogenetic biodiversity, in *Biological Diversity: Frontiers in Measurement and Assessment*, A. E. Magurran, B. J. McGill, Eds. (Oxford Univ. Press, 2011), pp. 194–207.

49. O. Purschke, S. G. Michalski, H. Bruelheide, W. Durka, Phylogenetic turnover during subtropical forest succession across environmental and phylogenetic scales. *Ecol. Evol.* **7**, 11079–11091 (2017). doi:10.1002/ece3.3564 Medline

50. B. Schmid, M. Baruffol, Z. Wang, P. A. Niklaus, A guide to analyzing biodiversity experiments. *J. Plant Ecol.* **10**, 91–110 (2017). doi:10.1093/jpe/rtw107

51. D. Butler, B. Cullis, A. Gilmour, B. Gogel, *Analysis of Mixed Models for S language Environments: ASReml–R Reference Manual* (Queensland DPI, 2007); www.vsni.co.uk/downloads/asreml/release2/doc/asreml-R.pdf.

52. eFloras (Missouri Botanical Garden, Harvard University Herbaria, 2017); www.efloras.org, http://frps.eflora.cn (accessed 22 December 2017).

53. Editorial Committee of Flora of Zhejiang, *Flora of Zhejiang* (Zhejiang Science and Technology Press, 1993).

54. G. Hu, K. J. Feeley, J. Wu, G. Xu, M. Yu, Determinants of plant species richness and patterns of nestedness in fragmented landscapes: Evidence from land-bridge islands. *Landsc. Ecol.* **26**, 1405–1417 (2011). doi:10.1007/s10980-011-9662-7

55. M. Yu, G. Hu, K. J. Feeley, J. Wu, P. Ding, Richness and composition of plants and birds on land-bridge islands: Effects of island attributes and differential responses of species groups. *J. Biogeogr.* **39**, 1124–1133 (2012). doi:10.1111/j.1365-2699.2011.02676.x

56. Y. Jin, H. Qian, M. Yu, Phylogenetic structure of tree species across different life stages from seedlings to canopy trees in a subtropical evergreen broad-leaved forest. *PLOS ONE* **10**, e0131162 (2015). doi:10.1371/journal.pone.0131162 Medline

57. Y. Jin, S. E. Russo, M. Yu, Effects of light and topography on regeneration and coexistence of evergreen and deciduous tree species in a Chinese subtropical forest. *J. Ecol.* **106**, 1634–1645 (2017). doi:10.1111/1365-2745.12911